e^+e^- Collisions

Richard Hemingway
Carleton University

16 April 1997

- Introduction
- Inclusive hadron production at LEP1
- Inclusive hadron production at LEP1.5-2
- Production of identified hadrons at LEP1
- Aspects of hadronisation:
  - Flavour separation
  - Leading particle effects
  - Quark-Gluon differences
  - Spin effects (polarisation,helicity)
  - Correlations in the di-baryon system
- Comparison with models
- Conclusions

INTRODUCTION

- ENORMOUS VOLUME OF WORK LEP (A,D,L,O) + SLD
- LEP1 COMPLETED → high statistics → refined studies
- LEP2 BEGINNING → small statistics → limited tests

- REVIEW SELECTED ASPECTS OF FRAGMENTATION OVER LAST 12-18 MONTHS

- REFS: 'INCLUSIVE PARTICLES AT LEP1' A. BOHRER SI-96-15

'QCD STUDIES WITH ALEPH' CERN-PPE 96-186

LAFFERTY, REEVES, WALLEY J. PHYS. G 21 (1995) A1 → DURHAM-RAL database

COMPILATION OF MULTIPLICITIES, OPAL TN350, R. HEMINGWAY April '97

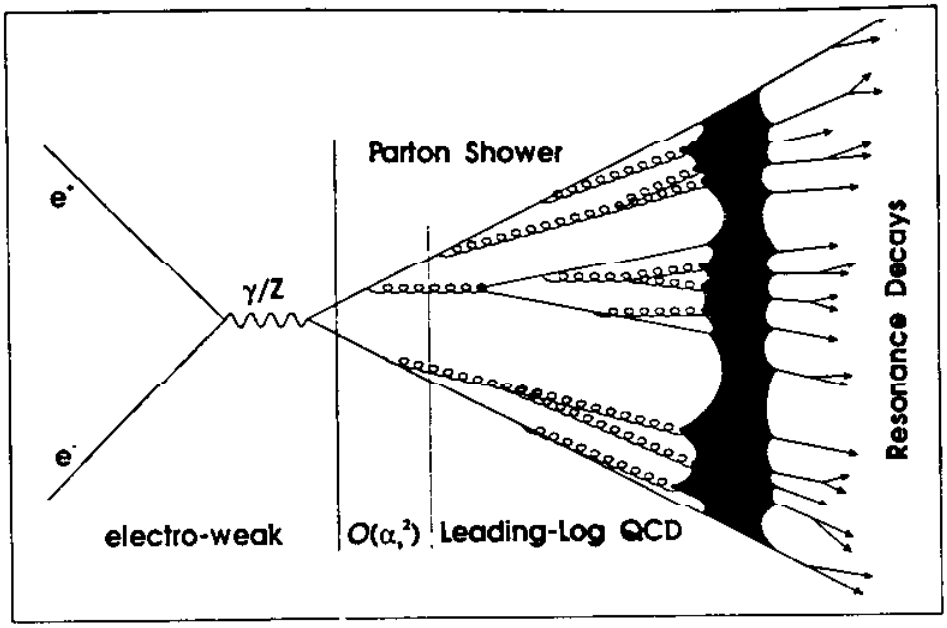

Figure 2.4: *Schematic view of a parton shower in e^+e^- annihilation with subsequent hadronization and particle decays [64].*

PARTON - HADRON FRAGMENTATION FUNCTIONS - formalism Nason + Webber

[1] - unpolarised beams, unpolarised outgoing hadrons $e^+e^- \to \gamma^*/Z \to \text{hadron} + X$

$$\frac{d^2\sigma}{dx\, d\cos\theta}(e^+e^- \to hX) = \frac{3}{8}(1+\cos^2\theta)\frac{d\sigma_T^h}{dx}(x,s) + \frac{3}{4}\sin^2\theta\frac{d\sigma_L^h}{dx}(x,s) + \frac{3}{4}\cos\theta\frac{d\sigma_A^h}{dx}(x,s)$$

where $\sigma_T, \sigma_L, \sigma_A$ are contributions from transverse polarisation γ/Z^*
longitudinal "
E-W parity violation

[2] - using perturbative QCD and factorisation, the above structure functions are convolutions of the parton fragmentation functions via

$$\frac{d\sigma_{T,L,A}^h}{dx} = \sum_{i=\text{partons}} \int_x^1 \frac{dz}{z} C_{T,L,A}^i(z, \mu^2/s)\, D_i^h(x/z, \mu^2)$$

C: coefficient fn's, calculable; μ^2: factorisation scale

[3] - energy dependence of D_i^h given by DGLAP evolution via

$$\frac{dD_j}{d\ln s}(x,s) = \sum_i \int_x^1 \frac{dz}{z} P_{ij}(z, \alpha_s(\mu), \mu^2/s)\, D_i(x/z, s)$$

P: Splitting kernels, calculable

OPAL, ALEPH, DELPHI via [1] → F_T, F_L

OPAL via [2] → Gluon Fragmentation F^g, in leading order QCD

ALEPH, DELPHI via [3] → Scaling Violation as $f^2\sqrt{s} \to \alpha_s$

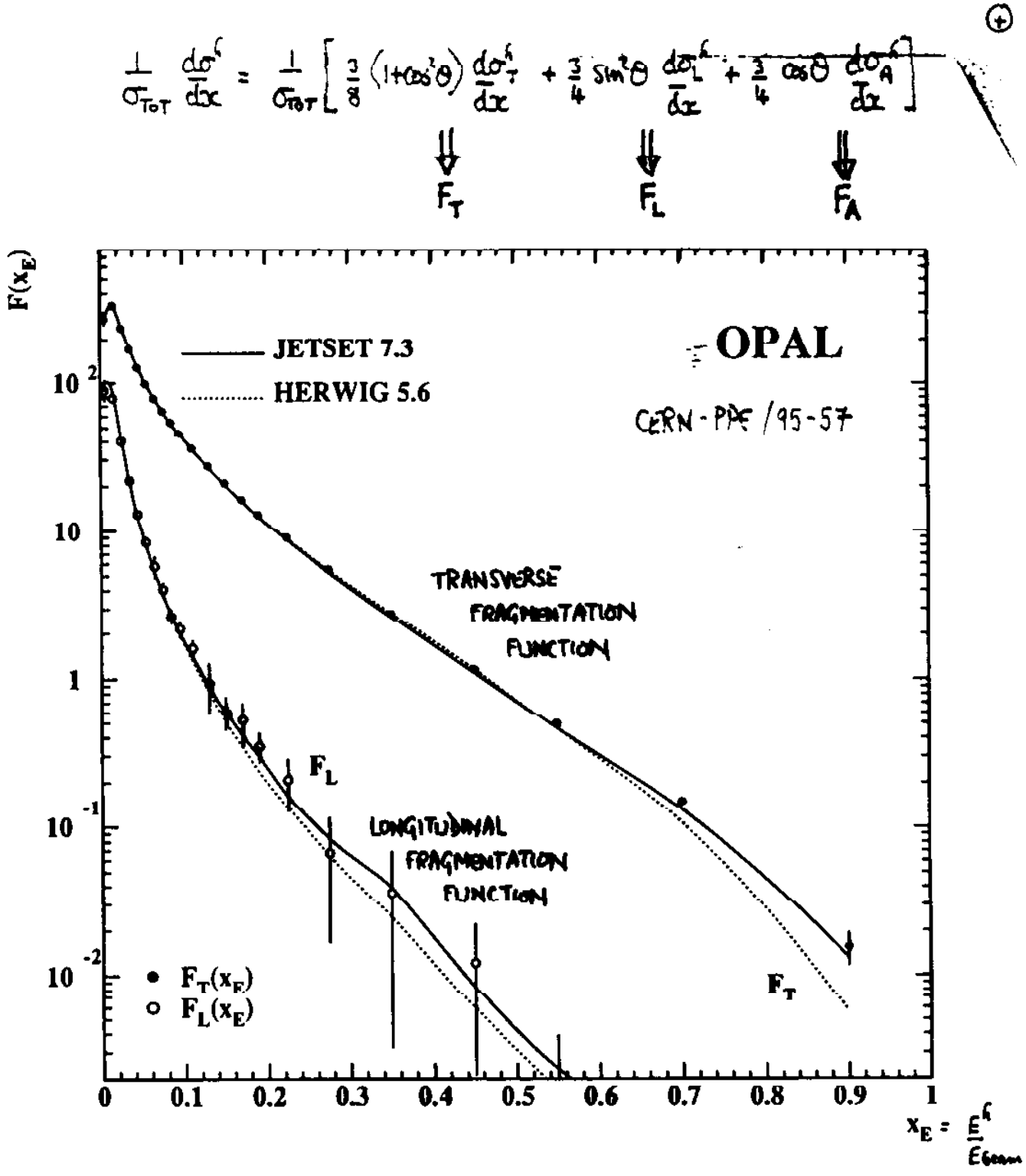

Figure 3: Measurements of $F_T(x)$ and $F_L(x)$ for charged particles; statistical and systematic errors are combined. The predictions of the QCD Monte Carlo programs JETSET and HERWIG are also shown. The data points are plotted at the bin centres, and the model predictions are averaged over the same bins and drawn as curves passing through the bin centres.

GLUON FRAGMENTATION FN

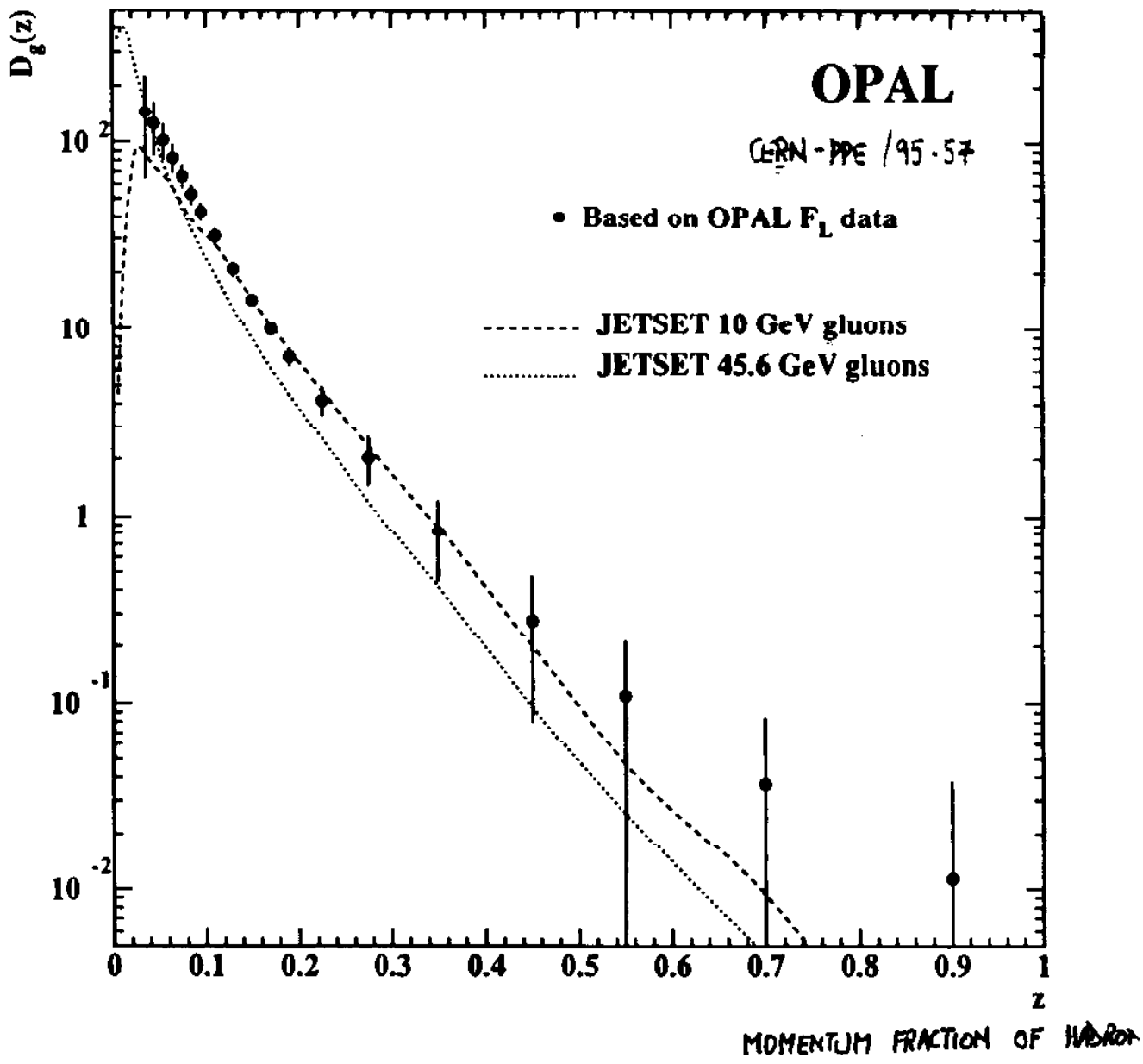

Figure 7: Gluon fragmentation function $D_g(z)$ for charged particles extracted from the longitudinal and transverse fragmentation functions. The errors include systematic contributions, and are highly correlated. Numerical values are given in Table 3. The predictions of the JETSET model for the fragmentation of gluon jets (in a gluon-gluon system) at two energies are shown.

CERN-PPE/95-096

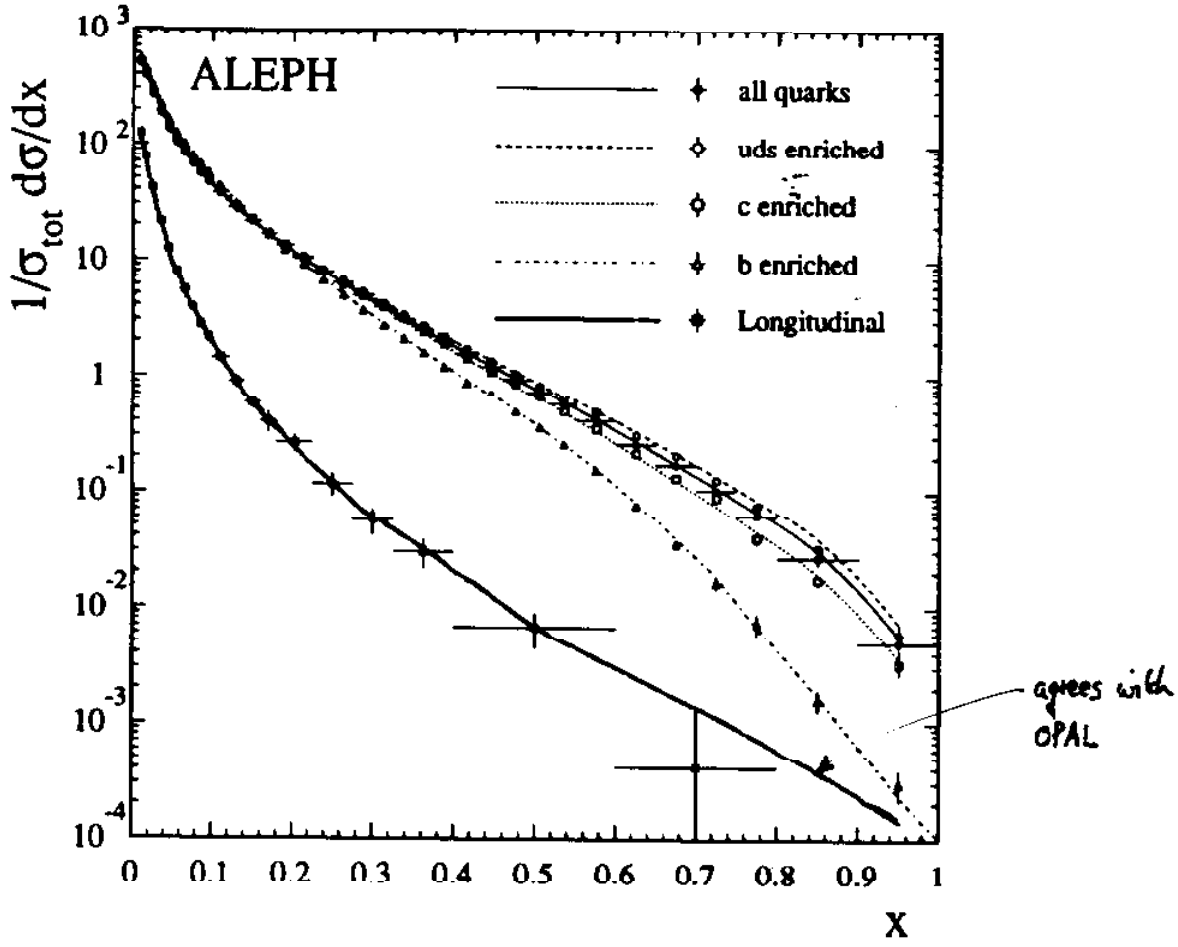

Figure 1: Measured scaled-energy distributions corrected for detector effects (symbols) and comparison with the predictions from JETSET 7.3 (curves). The distributions are normalized to the total number of events. Error bars include statistical and systematic uncertainties. The same binning is used for the inclusive and flavour-tagged distributions.

$\alpha_s(M_Z) = 0.126 \pm .007 \pm .006$

SCALING VIOLATIONS IN FRAGMENTATION FUNCTIONS

⇒ MEASUREMENT OF α_s

ALEPH CERN-PPE/95-096 and DELPHI CERN-PPE/96-185

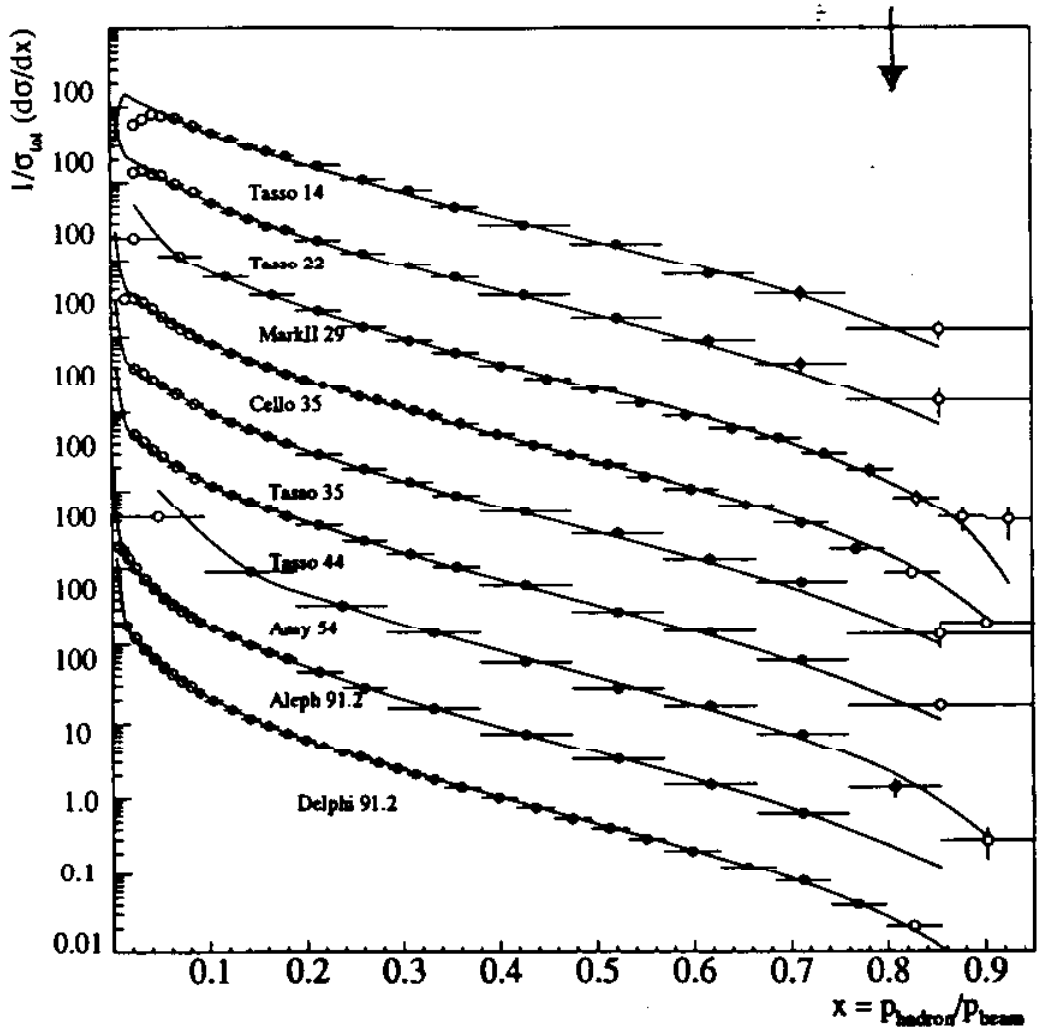

Figure 3: Inclusive scaled momentum distributions at centre-of-mass energies in the range between 14 GeV and 91.2 GeV. Only the full dots have been used in the fit.

$$\alpha_s(M_Z) = 0.124 \pm^{.006}_{.007} \pm .003$$

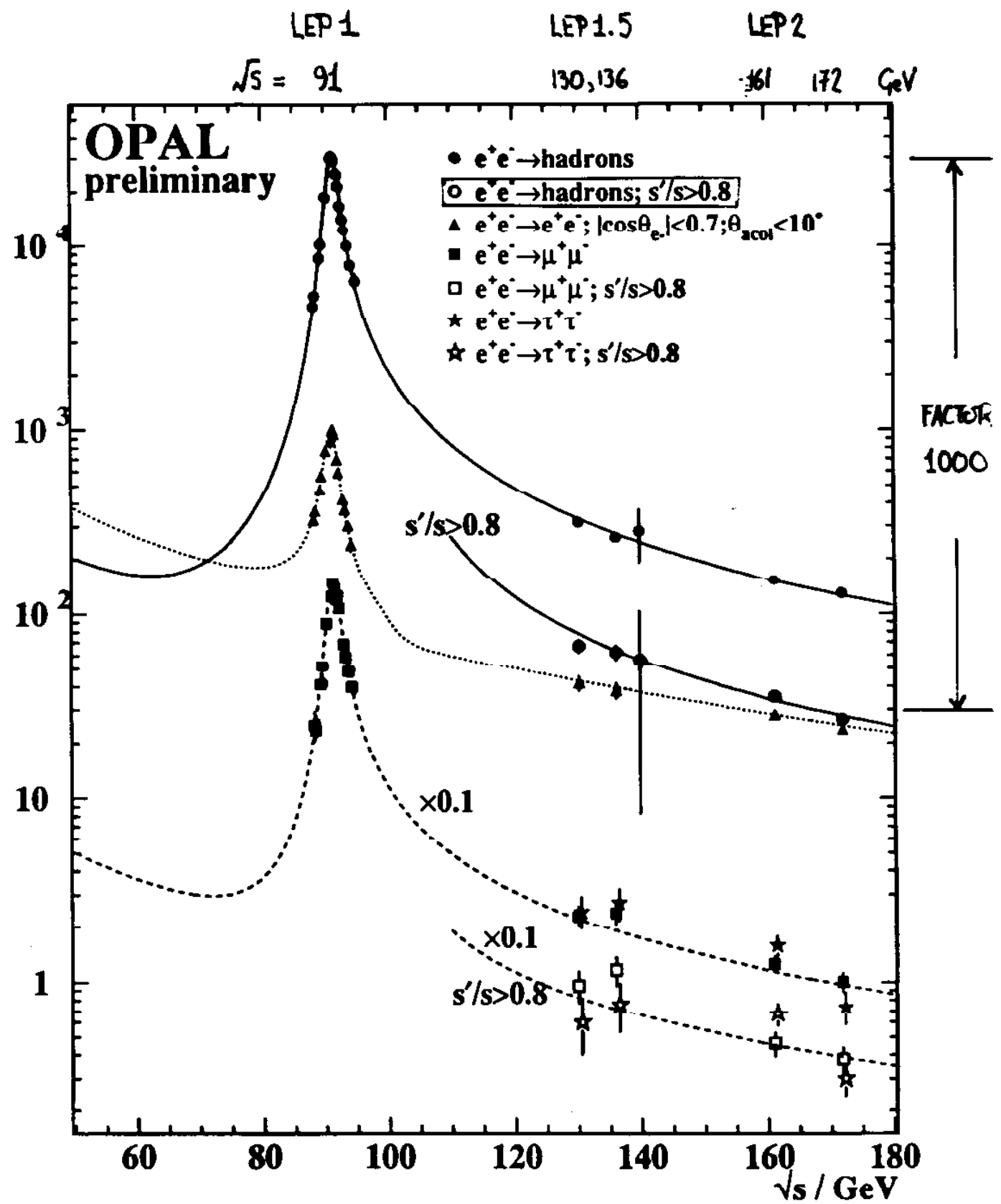
LEP 1
LEP 1.5
LEP 2
√s = 91
130, 136
161
172
GeV
OPAL
preliminary
e⁺e⁻→hadrons
e⁺e⁻→hadrons; s′/s>0.8
e⁺e⁻→e⁺e⁻; |cosθe⁻|<0.7; θacol<10°
e⁺e⁻→μ⁺μ⁻
e⁺e⁻→μ⁺μ⁻; s′/s>0.8
e⁺e⁻→τ⁺τ⁻
e⁺e⁻→τ⁺τ⁻; s′/s>0.8
FACTOR
1000
s′/s>0.8
×0.1
×0.1
s′/s>0.8
10⁴
10³
10²
10
1
60
80
100
120
140
160
180
√s / GeV

QCD TESTS AT LEP1.5 and LEP2

- See if QCD-based models/calculations give a good description of data

  [1] EVENT SHAPES, JET RATES - evolution with $\sqrt{s} \rightarrow \alpha_s$ (not discussed here)

  [2] CHARGED PARTICLES (a) Fragm. Fct $\frac{1}{\sigma}\frac{d\sigma^h}{d\xi}$ $\xi = \ln(1/x)$

  (b) Multiplicity Distrib^n

- LLA in QCD predicts
  - shape of ξ distrib^n [distorted Gaussian, peak ξ_0]
  - variation of ξ_0 with $\sqrt{s}$
  - variation of $\bar{n}_{ch}$ with $\sqrt{s}$

from talk by Emile Schyns (DELPHI) at Moriond-QCD 1997

Inclusive Charged Particle Production

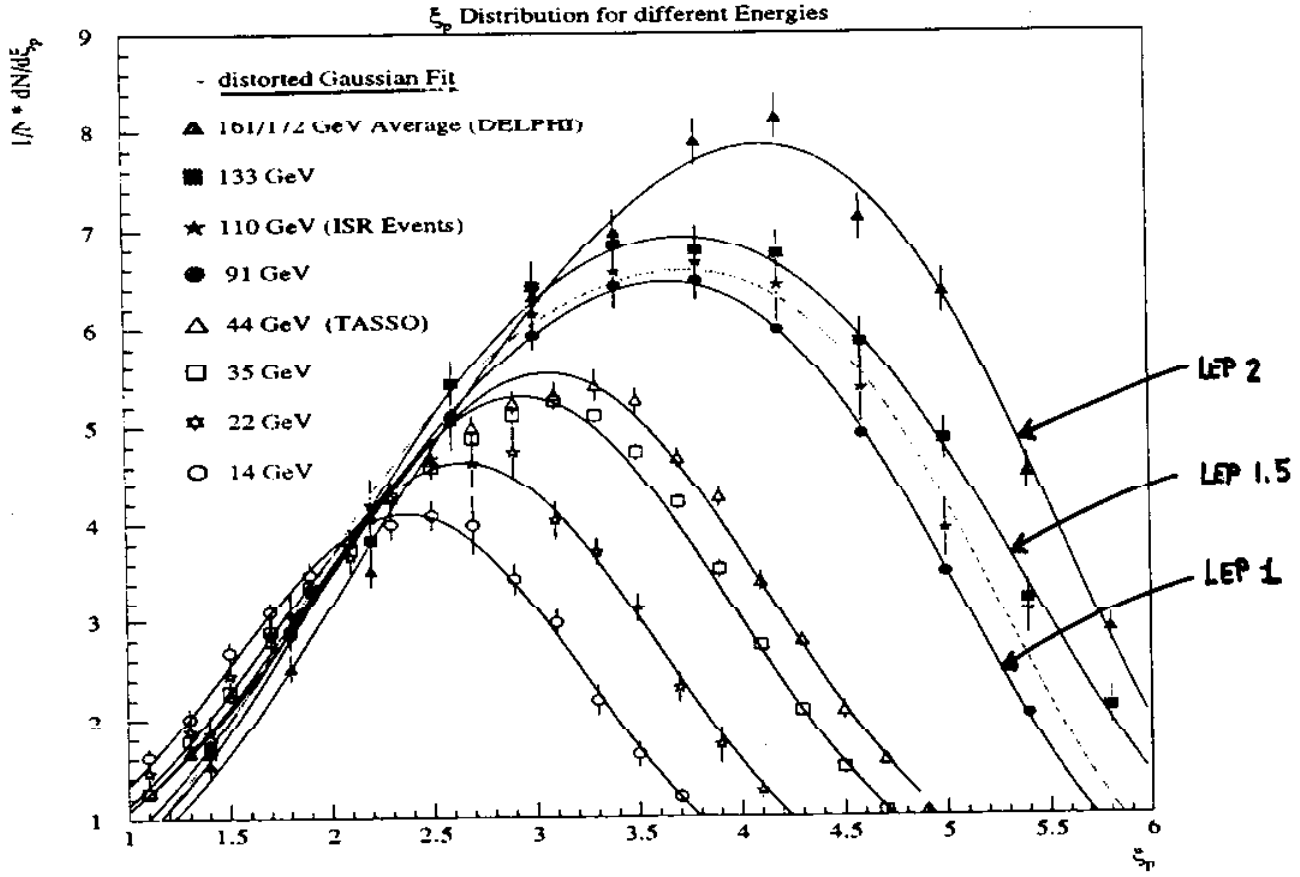

ALEPH , CERN-PPE/96-43

DELPHI , CERN-PPE/96-05 , CERN-PPE/96-130

OPAL-PN281 , CERN-PPE/97-15 , CERN-PPE/96-67

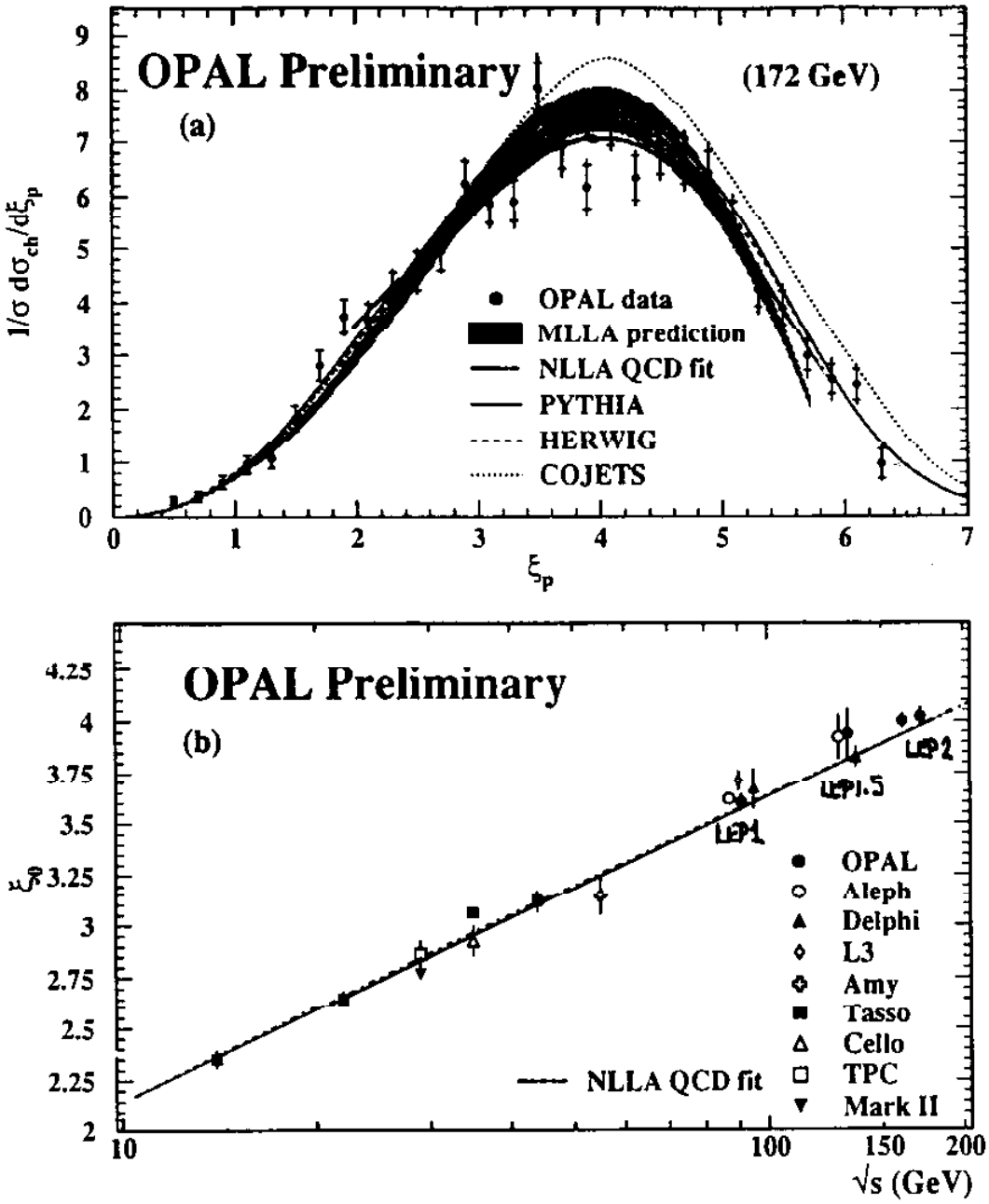

Figure 13: (a) Distribution of $\xi_p = \ln(1/x_p)$ for charged particles. Also shown are a fit of the NLLA QCD prediction, and predictions from MLLA QCD and PYTHIA, HERWIG and COJETS. The curve for the ARIADNE prediction is almost indistinguishable from the PYTHIA prediction and is omitted. (b) Evolution of the position of the peak of the ξ_p distribution, ξ_0, with the c.m. energy $\sqrt{s}$, compared with a fit of the NLLA QCD prediction up to and including the data at 161 GeV.

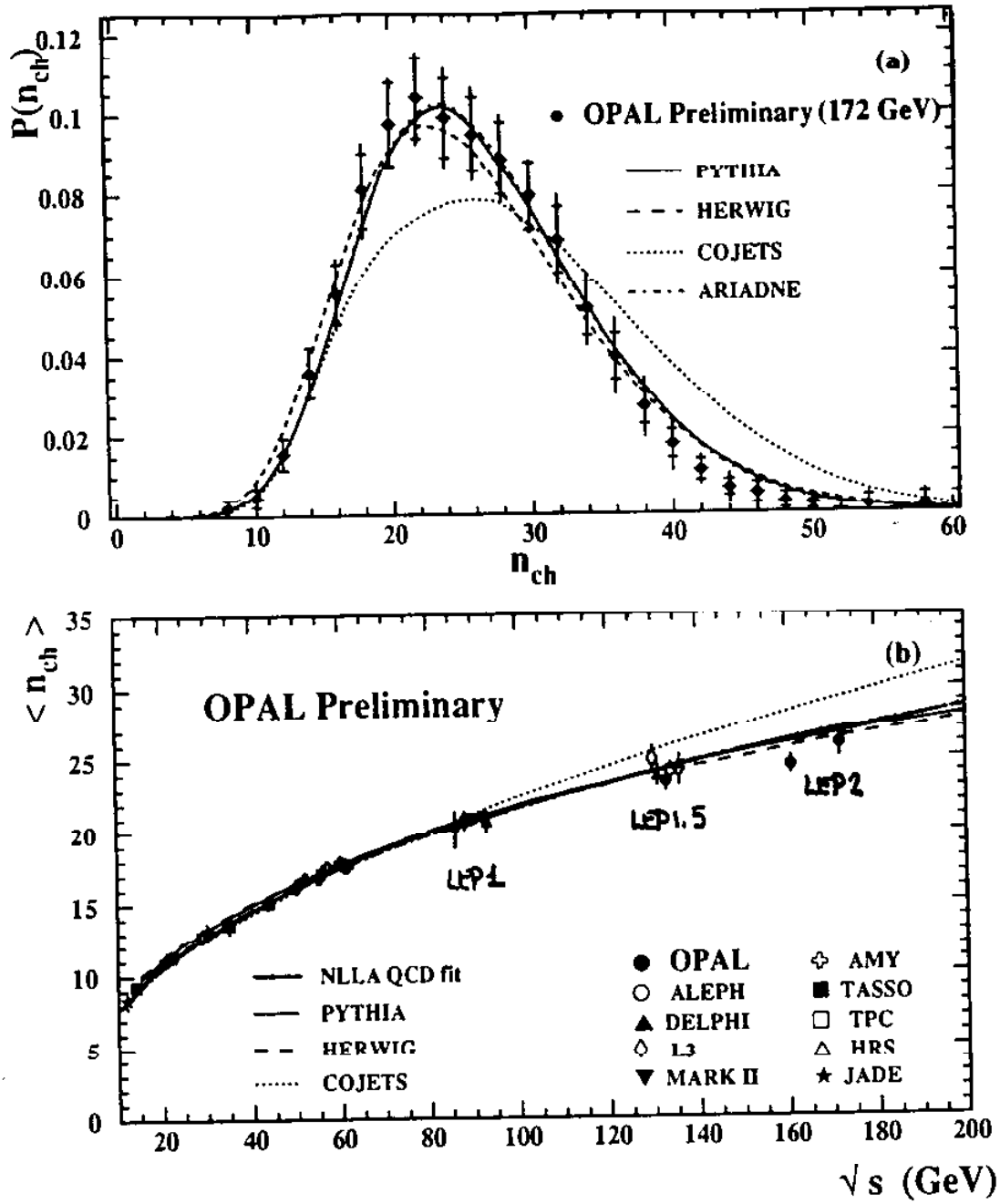

Figure 14: (a) Corrected distribution of the charged particle multiplicity n_{ch}. Predictions from PYTHIA, HERWIG, COJETS and ARIADNE are also shown. (b) Mean charged particle multiplicity measurements over a range of $\sqrt{s}$ from 12 GeV to 172 GeV. The measurements are compared to a fit of the NLLA QCD prediction for the evolution of the charged particle multiplicity with $\sqrt{s}$, up to and including the data at 161 GeV, and to the predictions from PYTHIA, HERWIG, and COJETS. The curve for the ARIADNE prediction is almost indistinguishable from the PYTHIA prediction and is omitted.

LATEST COMPILATION OF LEP1 INCLUSIVE RATES

- OPAL TN350 (4 April 1997)

Particle	J^P	Experiment	Reference	Rate/event Measured	Rate/ev JT7.4 +MOPS	Rate/ev HW5.9
All charged		M,A,D,L,O	[11, 15, 31, 32, 33] [54, 59, 64, 84]	20.924 ± 0.117	21.160	20.945
γ	1^-	A	[30]	21.38 ± 0.70	21.170	20.520
π^0	0^-	A,D,L	[28, 48, 54, 60]	9.83 ± 0.26	9.881	9.624
$\pi^\pm$	0^-	O	[72]	17.05 ± 0.43	17.652	16.927
η	0^-	A,L	[30, 25, 60]	0.962 ± 0.053	0.872	0.841
$\rho(770)^0$	1^-	A,D	[25, 40]	1.295 ± 0.125	1.445	1.098
$\omega(782)$	1^-	A,L	[25, 62]	1.108 ± 0.111	1.940*	1.077
$\eta'(958)$	0^-	A	[30, 62]	0.163 ± 0.058	0.151	0.133
$f_0(980)$	0^+	D,L	[40, 58]	0.144 ± 0.021	0.093	0.089
$a_0(980)$	0^+	L	[58]	0.14 ± 0.06	0.100	0.102
$\phi(1020)$	1^-	A,D,O	[25, 52, 73]	0.108 ± 0.006	0.099	0.113
$f_2(1270)$	2^+	D,L	[40, 58]	0.239 ± 0.050	0.176	0.156
$f_2'(1525)$	2^+	D	[51]	0.020 ± 0.008	0.015	0.029
$K^\pm$	0^-	D,O	[38, 72]	2.365 ± 0.105	2.157	2.134
K^0	0^-	S,A,D,L,O	[19, 34, 40, 57, 83, 12]	2.027 ± 0.025	2.075	2.029
$K^*(892)^\pm$	1^-	A,D,O	[30, 34, 40, 71]	0.731 ± 0.058	0.770	0.782
$K^*(892)^0$	1^-	A,D,O	[25, 35, 52, 73]	0.761 ± 0.032	0.780	0.778
$K_2^*(1430)^0$	2^+	D,O	[52, 73]	0.106 ± 0.060	0.081	0.119
$D^\pm$	0^-	A,D,O	[18, 43, 85]	0.191 ± 0.021	0.184	0.176
D^0	0^-	A,D,O	[18, 43, 85]	0.482 ± 0.025	0.507	0.457
$D_s^\pm$	0^-	A,O	[27, 85]	0.129 ± 0.013	0.094	0.106
$D^*(2010)^\pm$	1^-	A,D,O	[18, 43, 76]	0.183 ± 0.010	0.237*	0.206
J/Ψ	1^-	A,D,L,O	[24, 39, 61, 67, 79]	$(5.40 \pm 0.31)10^{-3}$	0.00577	0.00527
χ_{c1}	1^+	D,L	[39, 61]	$(4.3 \pm 1.2)10^{-3}$	0.0015	0.0012
$\Psi(3685)$	1^-	D,O	[39, 79]	$(2.29 \pm 0.47)10^{-3}$	0.0009	0.0008*
$\Upsilon(9460)$	1^-	O	[80]	$(1.43 \pm 0.65)10^{-4}$		
p	$\frac{1}{2}^+$	D,O	[38, 72]	0.977 ± 0.087	0.836	1.379*
Δ^{++}	$\frac{3}{2}^+$	D,O	[47, 81]	0.088 ± 0.034	0.109	0.261*
Λ	$\frac{1}{2}^+$	A,D,L,O	[19, 34, 37, 57, 86]	0.373 ± 0.008	0.359	0.774*
Σ^+	$\frac{1}{2}^+$	O	[87]	0.099 ± 0.015	0.075	0.119
Σ^0	$\frac{1}{2}^+$	A,D,O	[30, 46, 87]	0.074 ± 0.009	0.071	0.100
Σ^-	$\frac{1}{2}^+$	O	[87]	0.083 ± 0.011	0.067	0.103
Ξ^-	$\frac{1}{2}^+$	A,D,O	[30, 34, 45, 86]	0.0262 ± 0.0010	0.0280	0.1285*
$\Sigma(1385)^\pm$	$\frac{3}{2}^+$	A,D,O	[30, 45, 86]	0.0471 ± 0.0046	0.0561	0.2328*
$\Xi(1530)^0$	$\frac{3}{2}^+$	A,D,O	[30, 45, 86]	0.0058 ± 0.0010	0.0063	0.0693*
Ω^-	$\frac{3}{2}^+$	A,D,O	[30, 46, 86]	0.00125 ± 0.00024	0.00105	0.03154*
Λ_c^+	$\frac{1}{2}^+$	D,O	[49, 85]	0.076 ± 0.015	0.056	0.095
$\Lambda(1520)$	$\frac{3}{2}^-$	O	[86]	0.0213 ± 0.0028		

note later

38 SPECIES

L=1 baryon

Table 1: Particle Production rates at 91.21 GeV compared with OPAL-tuned versions of JETSET74+MOPS and HERWIG59. The experiments are Aleph(A), Delphi(D), L3(L), Opal(O), MK2(M), and SLD(S). Particle and anti-particle rates are summed and sequential particle decay is activated. * indicates that the rate differs from measurement by more than three standard deviations.

COMPILATION : LAFFERTY/REEVES/WHALLEY J. Phys. G 21 (1995) A1

EXAMPLE 1 $\frac{1}{\sigma_{had}} \frac{d\sigma}{dx_p}$ FOR $e^+e^- \to hadrons^{\pm} + X$

DURHAM-RAL HEP database

Compilation of e^+e^- data: fragmentation functions

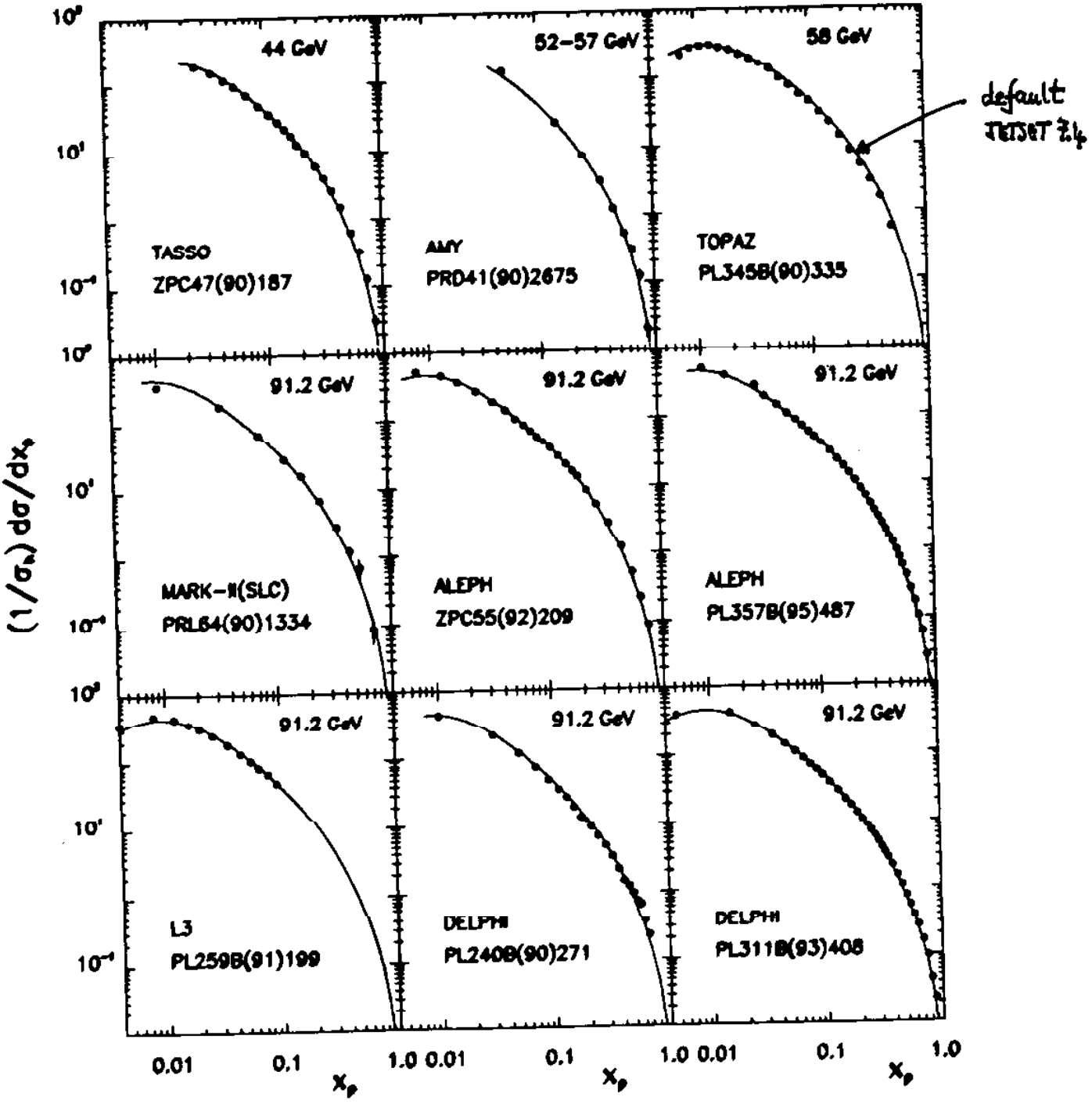

Figure 5. (continued).

EXAMPLE 2 $\frac{1}{\sigma_{had}} \frac{d\sigma}{dx_p}$ FOR $e^+e^- \to K^0(\bar{K}^0) + X$

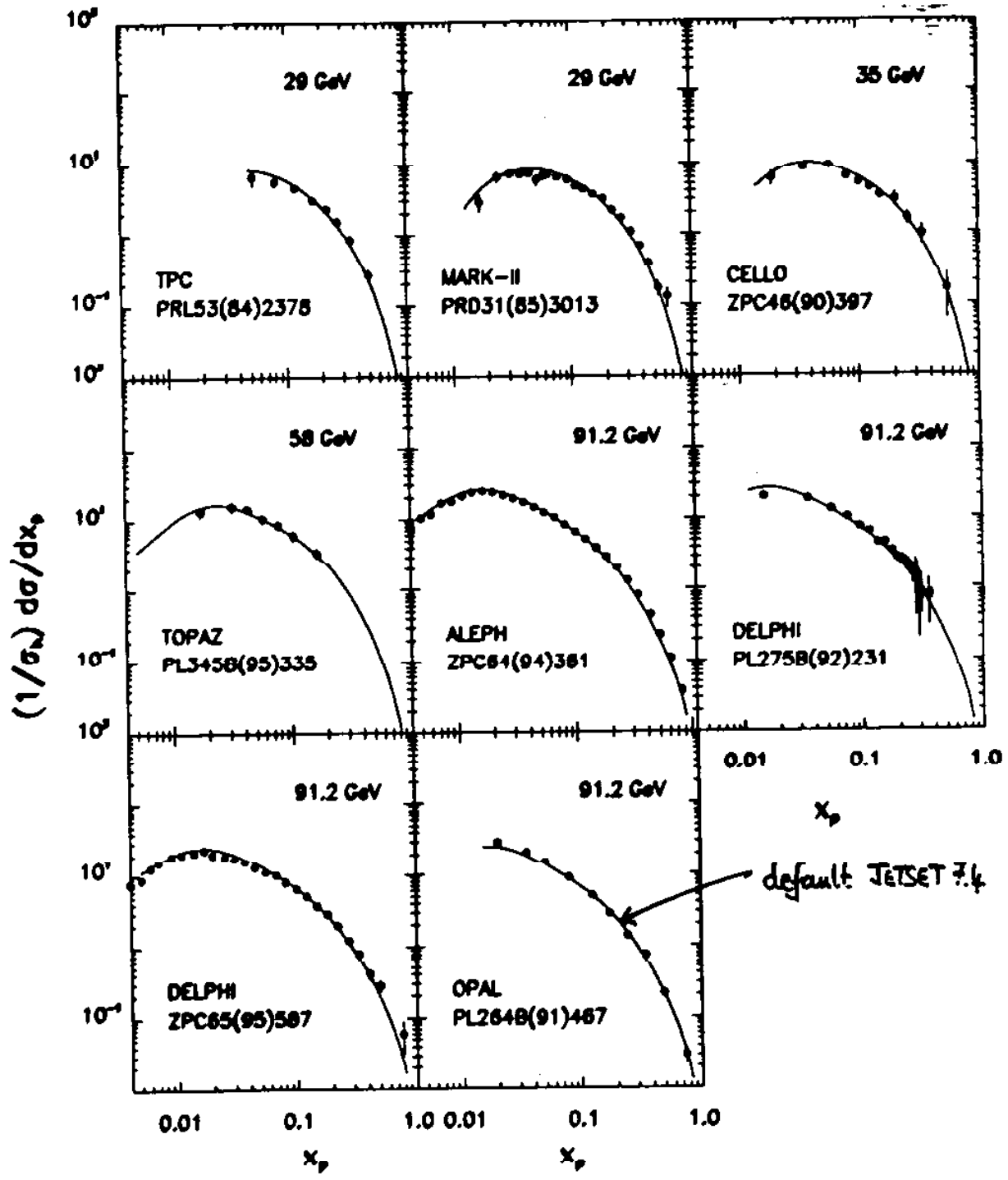

Figure 24. Distributions in $(1/\sigma_h)\, d\sigma/dx_p$ for $e^+e^- \to K^0(\bar{K}^0)\, X$.

EXAMPLE 3 $\frac{1}{\sigma_{had}} \frac{d\sigma}{dx_p}$ FOR $e^+e^- \to \Lambda(\bar{\Lambda}) + X$

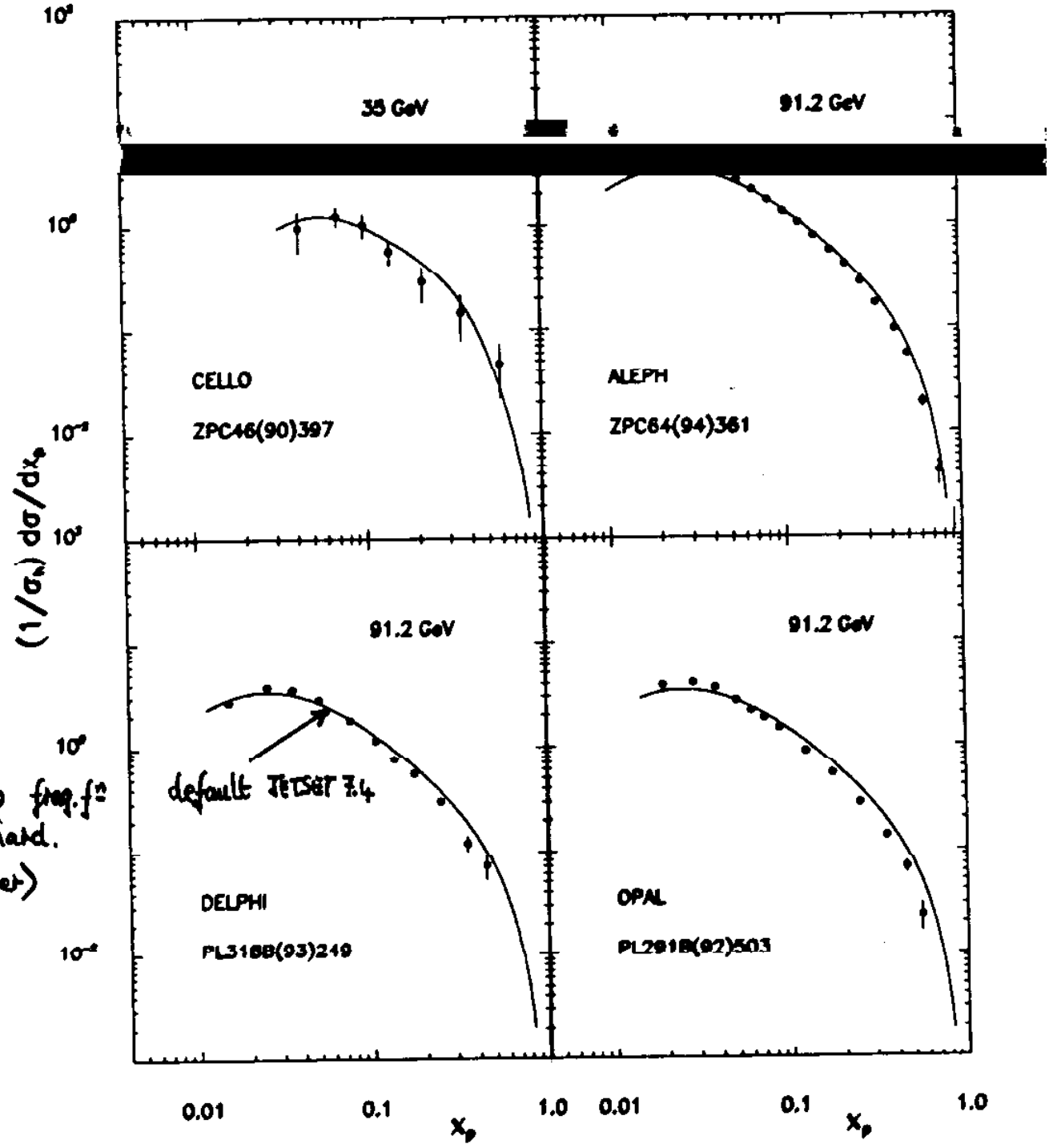

PROBLEM!

MONTECARLO freq. f° is too hard. (see later)

Figure 39. Distributions in $(1/\sigma_h)\, d\sigma/dx_p$ for $e^+e^- \to \Lambda(\bar{\Lambda})\, X$.

FLAVOUR SEPARATION - based on Nº tks with $d_0/\sigma_{d_0} > 3$ = N_{sig}

Light Quarks	6-Quarks
$N_{sig} = 0$	$N_{sig} \geq 3$
Purity ~ 86%	Purity ~ 90%

Figure 6: Hadronic Spectra in $Z^0 \rightarrow uu, dd, ss$ Decays

(SLD Preliminary) SLAC-PUB-7199

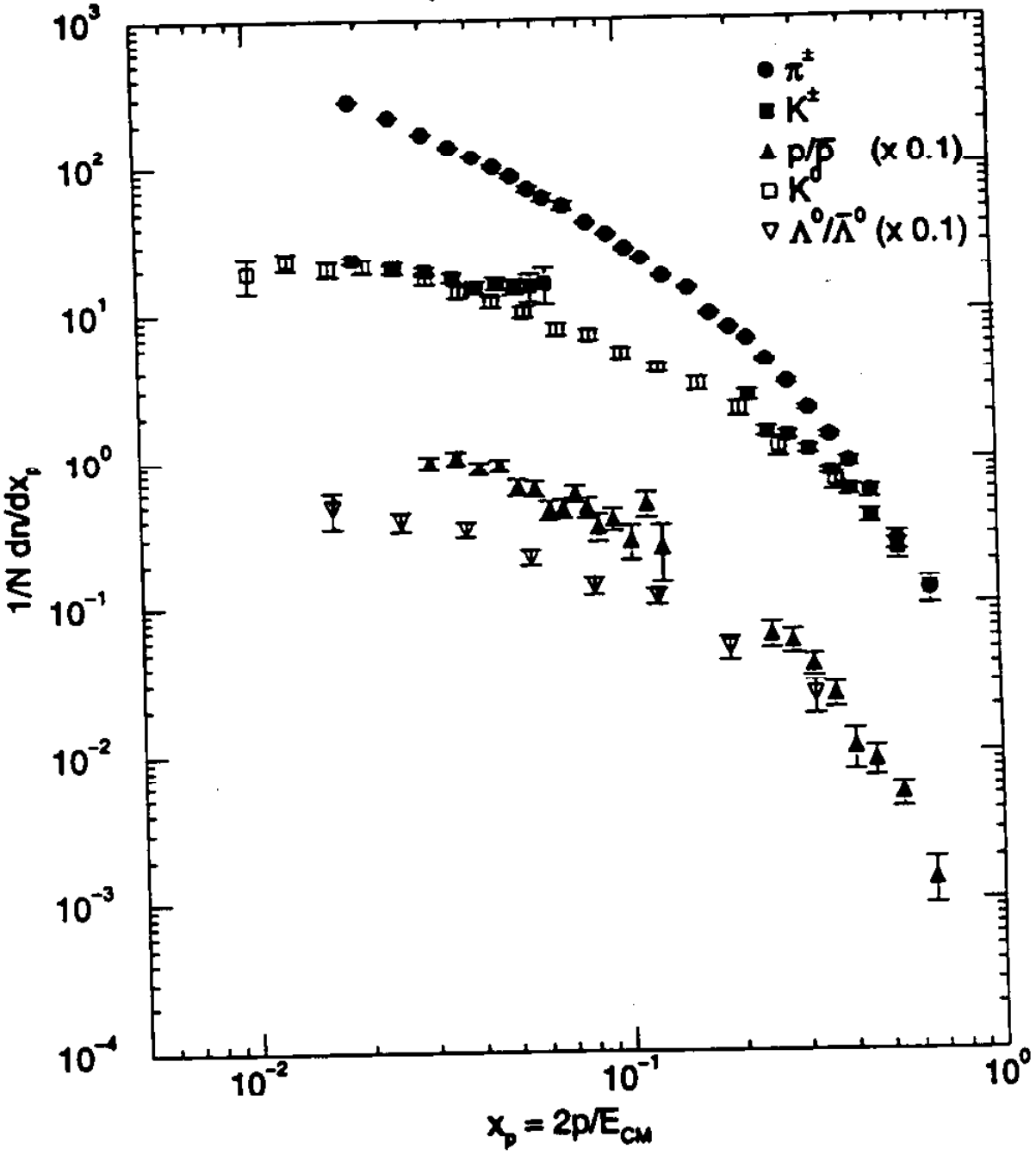

SLAC-PUB-7199

Figure 7: *b/uds* Production Ratio

SLD - Preliminary

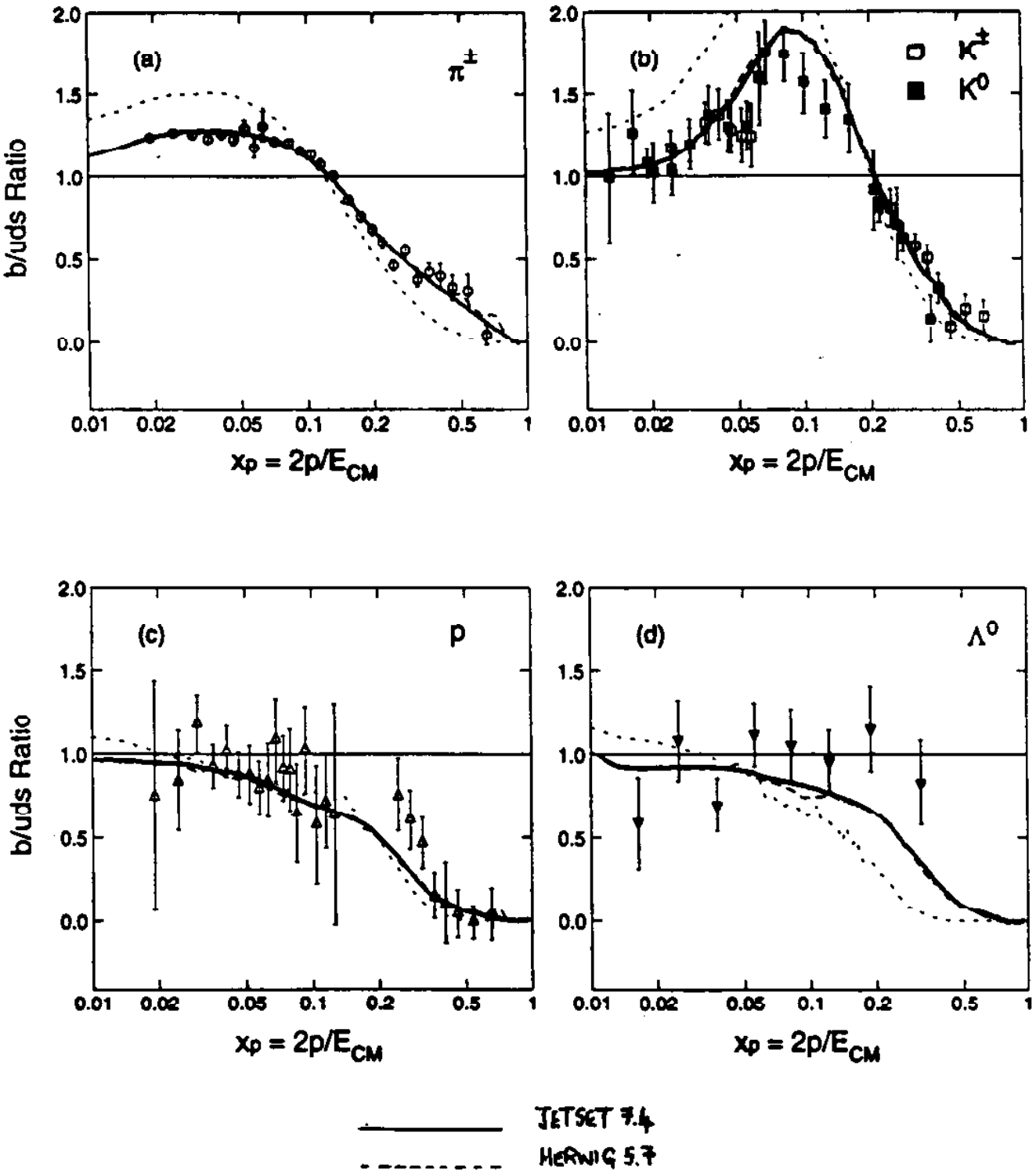

LEADING PARTICLE EFFECTS

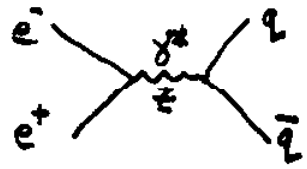

In SM quark prefers e^-_L direction

$$\frac{d\sigma}{d\cos\theta} \sim 1 + \cos^2\theta + 2A_q A_z \cos\theta$$

where $A_z = \frac{A_e - P_e}{1 - A_e P_e}$

With SLC $\Rightarrow |P_e| \sim 0.7$

$\Rightarrow A_z > A_e$

ie $A_z^{SLC} > A_z^{LEP}$

Require events with $N_{sig} = 0$

$\Rightarrow$ high purity (u,d,s) events

With e^-_L and $|\cos\theta| > 0.2$

$\Rightarrow$ 73% quarks

expect more K^- than K^+

p than $\bar{p}$

SLD COLLABORATION

SLAC-PUB-7197
and -7395

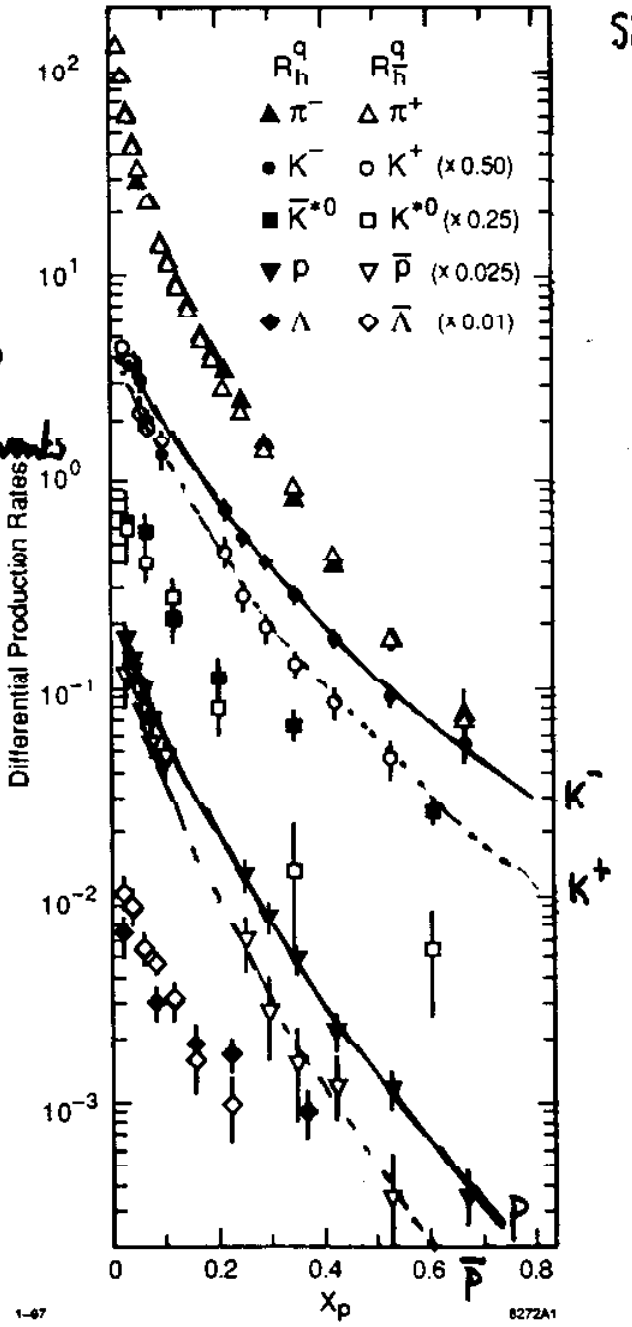

Figure 1: Differential production rates as a function of scaled momentum. The ordinates represent average multiplicities per light quark jet per unit interval in scaled momentum.

QUARK-GLUON JET DIFFERENCES

- SELECT 3-JET EVENTS
- ENERGY ORDER

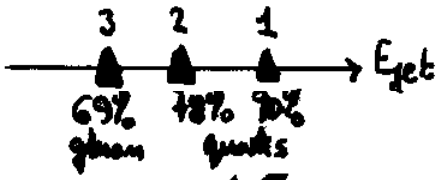

L3 - CERN-PPE/95-182

$\pi^0, \eta \to \gamma\gamma$

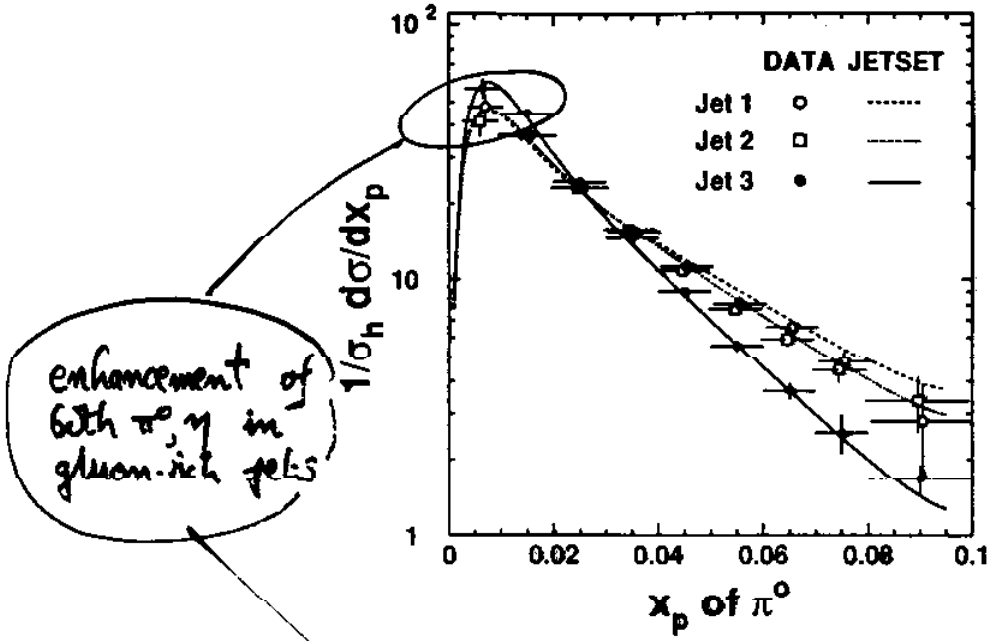

enhancement of both π^0, η in gluon-rich jets

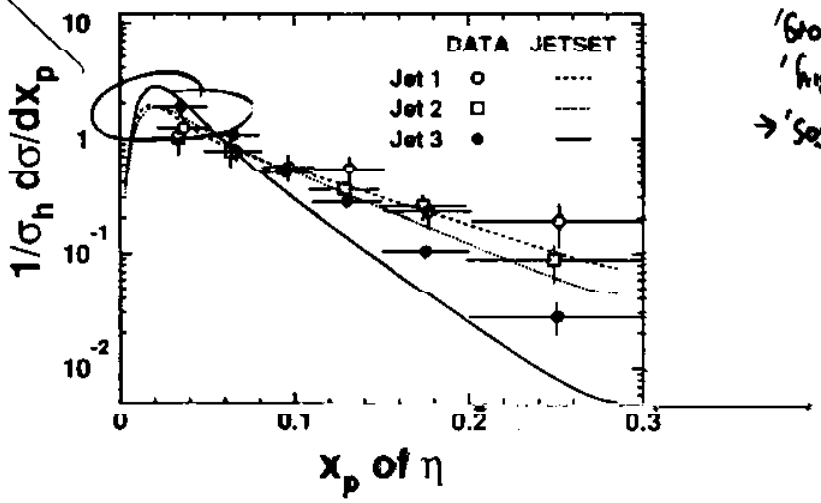

Observation is consistent with other knowledge - viz GLUON jets are 'broader' and have 'higher' multiplicity, → 'softer' spectrum.

Figure 7.17: *The π^0 and η momentum spectrum in quark and gluon enriched jets. The data are compared with the prediction of the* JETSET *Monte Carlo [155].*

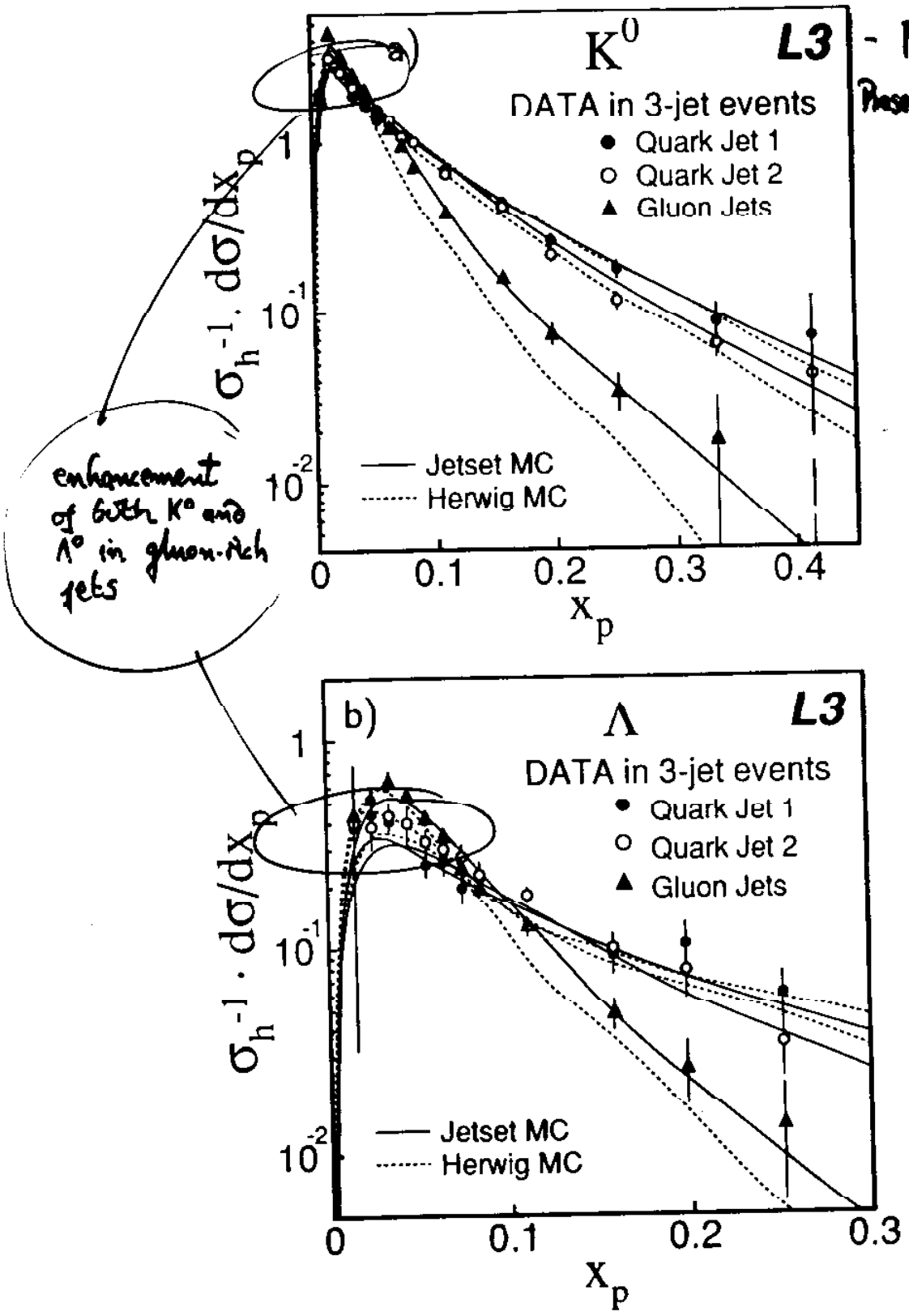

- preliminary

Presented at Moriond-97

enhancement of both K^0 and Λ^0 in gluon-rich jets

QUESTION: DOES THE ENHANCEMENT SCALE WITH CHARGED MULTIPLICITY?

DEFINE $R = \langle K^0_S \rangle_{jet} / \langle N_{ch} \rangle_{jet} \Big/ \langle K^0_S \rangle_{total} / \langle N_{ch} \rangle_{total}$

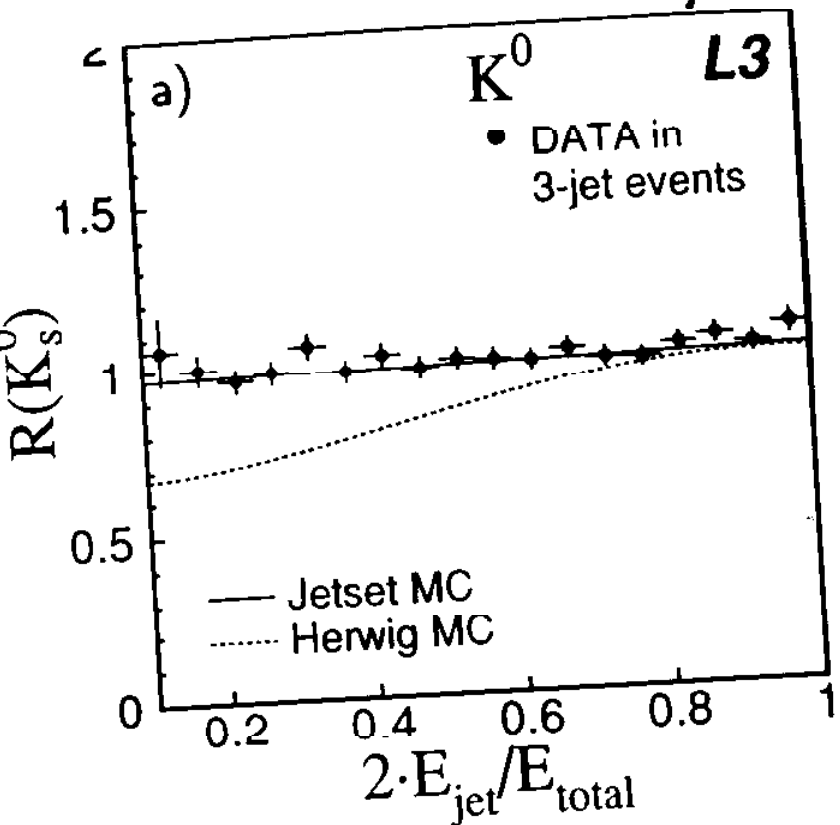

NB JETSET tracks trends.

SIGNIFICANT INCREASE IN Λ^0 PRODUCTION wrt CHARGED IN GLUON-RICH JETS.

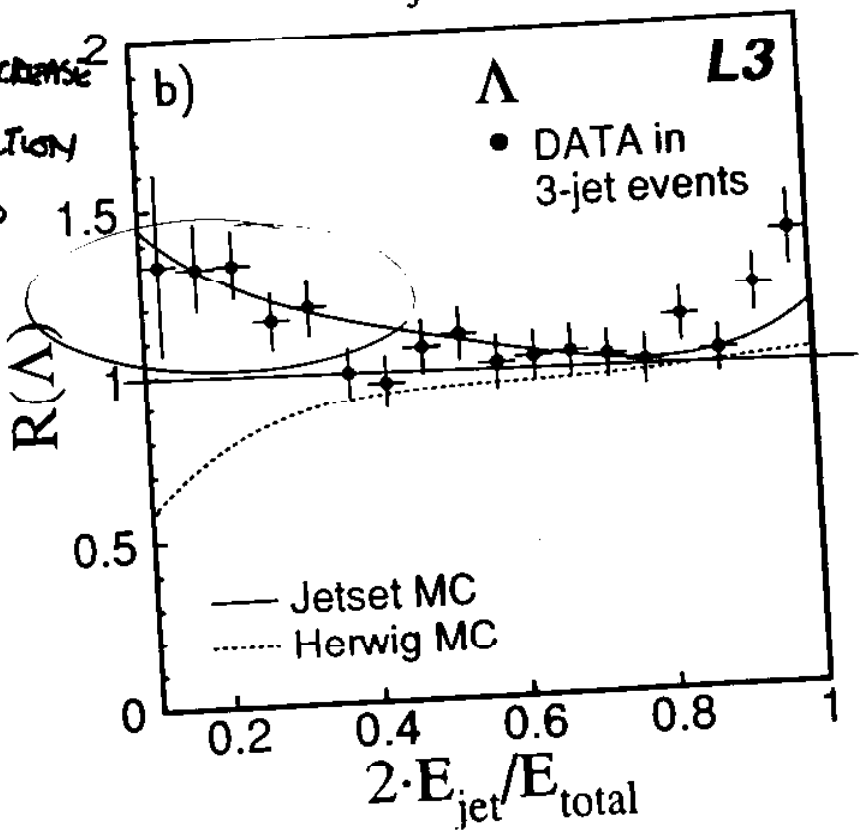

3 JET, ENERGY ORDERING

OPAL PN 236, JLY 96
→ SUMMER CONFERENCES

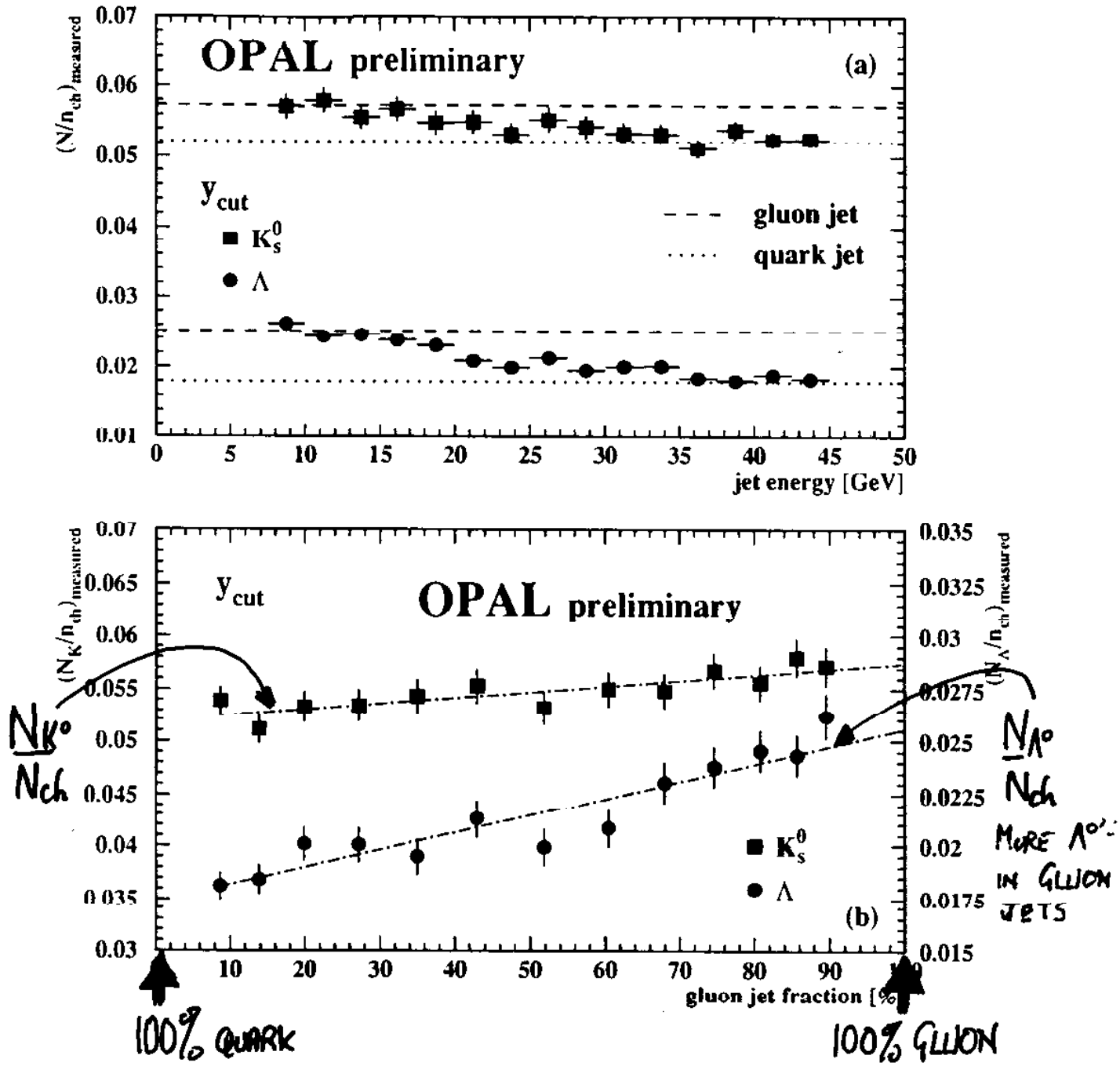

Figure 4: Relative Λ and K^0_s rates for the y_{cut} selection. The errors are statistical.
(a) $R^\Lambda(E_{jet}) = N_\Lambda/n_{ch}(E_{jet})$ and $R^K(E_{jet}) = N_K/n_{ch}(E_{jet})$ as function of the jet energy. The lines show the results for true quark and gluon jets as obtained by the fit.
(b) $R^\Lambda(p_g) = N_\Lambda/n_{ch}(p_g)$ and $R^K(p_g) = N_K/n_{ch}(p_g)$ as function of the gluon jet fraction p_g. The lines indicate the results of the extrapolation.

3 JET EVENTS - Υ

DELPHI

CERN-PPE/96-193

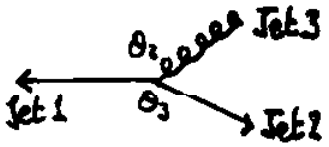

⇒ Identified Particles $K^{\pm}, p, K^{0}, \Lambda^{0}$ as f = mom

$\theta_2 \sim \theta_3 \sim 150°$

b-tag → quark

$$R(p) = \frac{[\text{RATE}/n_{ch}]_{\text{GLUON}}}{[\text{RATE}/n_{ch}]_{\text{QUARK}}}$$

Normalized ratios

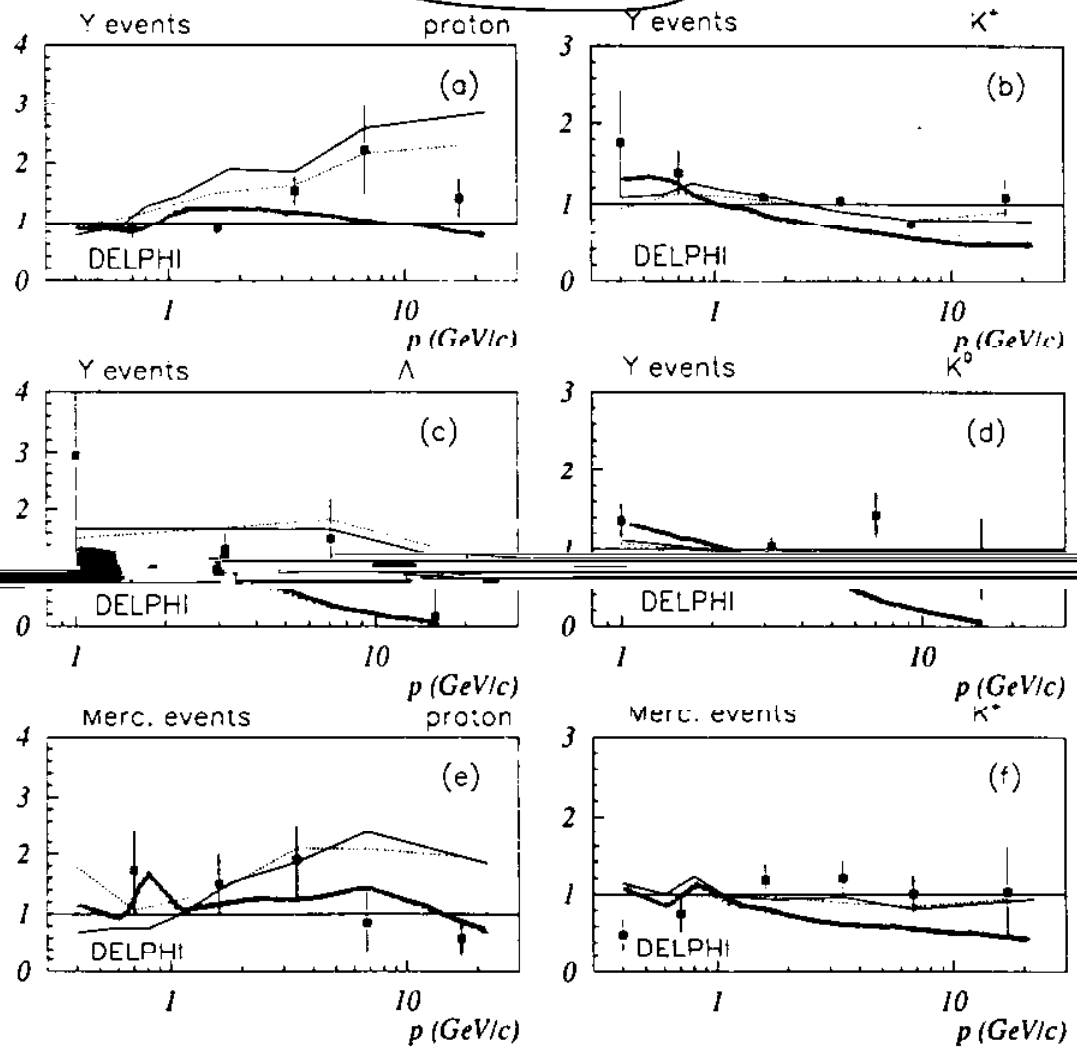

Reasonable tracking & MCs ?

Figure 5: *As Fig. 3. but for the normalized ratio. $R'_X(p)$ defined in the text (black squares), and the corresponding model predictions.*

HERWIG 5.8 ——— JETSET 7.4 ——— 7.3 .....

SPIN EFFECTS - POLARISATION

Polarisation ~ -0.91 ± .01

Leading Λ^0 QUARK MODEL $\Lambda^{\uparrow} = [u^{\uparrow}d^{\downarrow}]s^{\uparrow}$

ALEPH - CERN-PPE/96-04

LAMBDA LONGITUDINAL POLARISATION

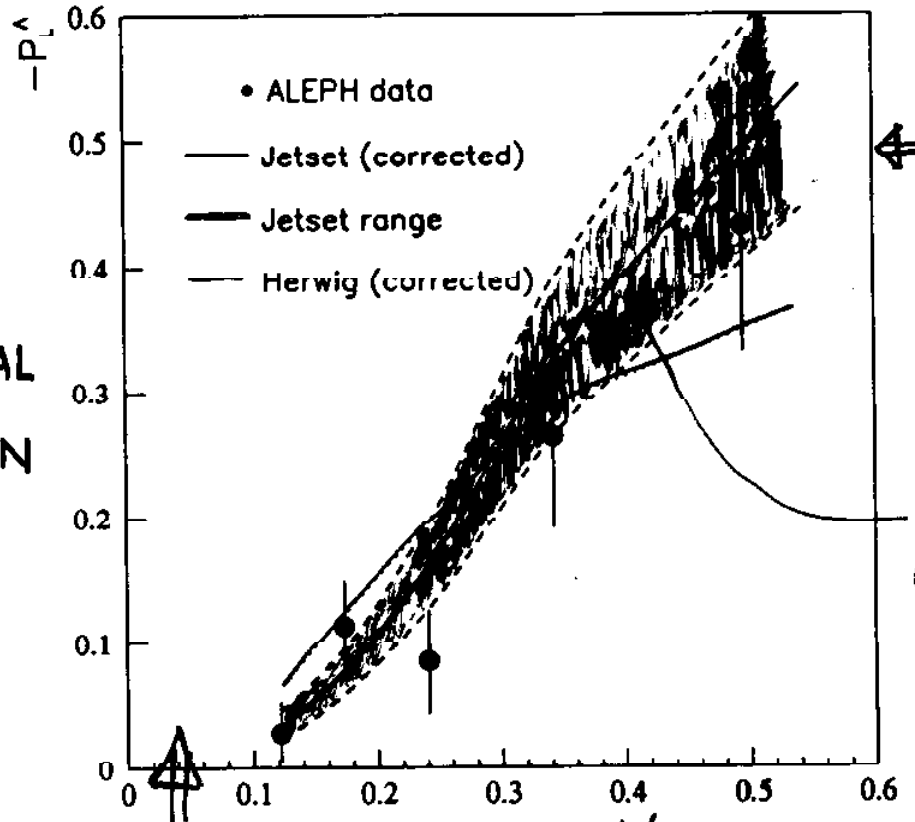

Large polarisation at large z

JETSET + QUARK M

Gustafson + Hakkine

Small polarisation at small z

Figure 3: The measured longitudinal Λ polarization is shown as dots. The JETSET prediction after multiplying by a correction factor of 1.07 is shown as a solid line. The dashed lines indicate the estimated uncertainty of the JETSET prediction. The HERWIG prediction after multiplication by a correction factor of 2.17 is shown as a dotted line.

SPIN EFFECTS - HELICITY DENSITY MATRIX

INCLUSIVE PRODUCTION OF VECTOR MESONS $(J^P = 1^-)$ $M = \begin{matrix} +1 \\ 0 \\ -1 \end{matrix}$

- $\phi \to K\bar{K}$, $D^{*\pm} \to D\pi$, $B^* \to B\gamma$ OPAL

- DECAY DISTRIB $\Rightarrow$ elements of density matrix ρ_{mm}

ϕ, D^* $\quad W(\cos\theta_h) = \frac{3}{4}\left[(1-\rho_{00}) + (3\rho_{00}-1)\cos^2\theta_h\right]$

B^* $\quad W(\cos\theta_h) = \frac{1}{2}\left[1 - \frac{3\rho_{00}-1}{4}(3\cos^2\theta_h - 1)\right]$

- ALIGNMENT $\eta = \frac{3\rho_{00}-1}{2}$ $\quad \therefore \rho_{00} = 1/3$ implies no spin alignment

	ρ_{00}
ϕ	0.54 ± 0.08
$\to D^*$	0.40 ± 0.02
$\to D^*$	0.34 ± 0.03
B^*	0.36 ± 0.09

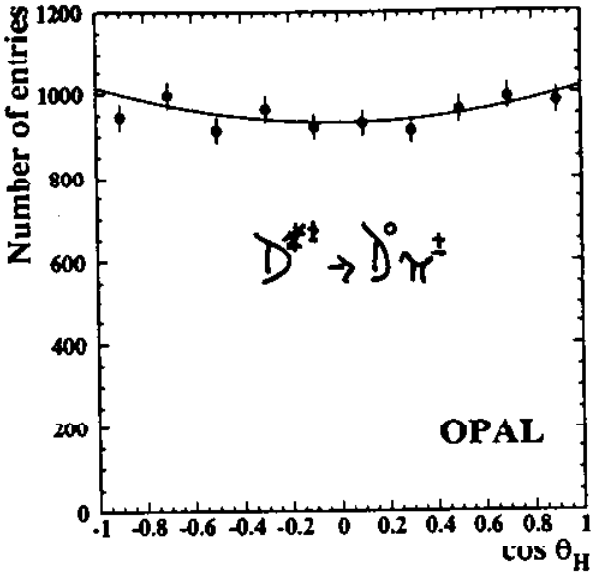

CERN-PPE/97-05

Figure 4: The $\cos\theta_H$ distribution of all D^* candidates. The result of the 3 parameter log-likelihood fit for the spin alignment has been superimposed.

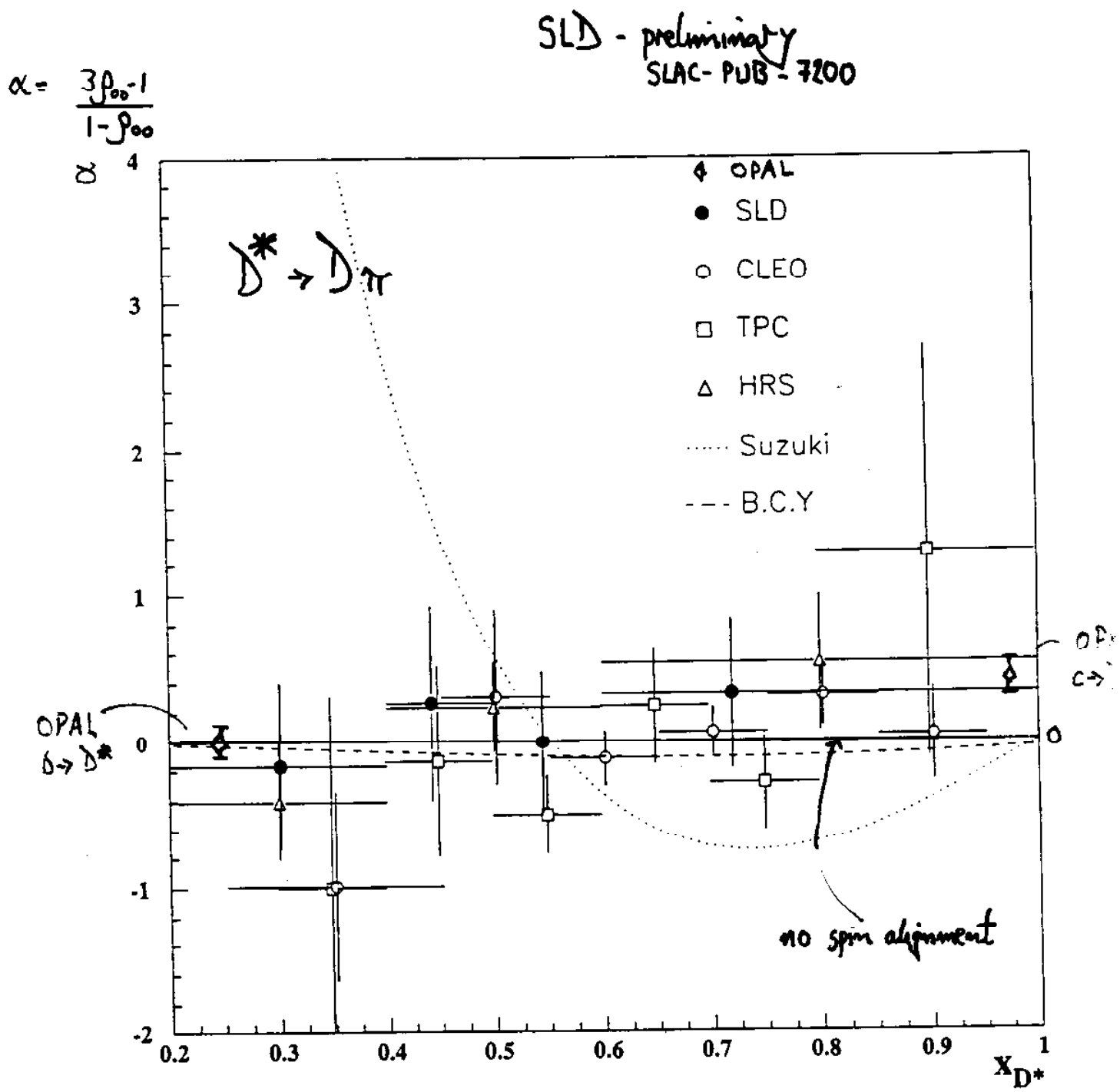

Figure 4: Fitted α as a function of x_{D^*} together with CLEO, HRS, and TPC data from lower *c.m.* energies. Model calculations are also shown (see text).

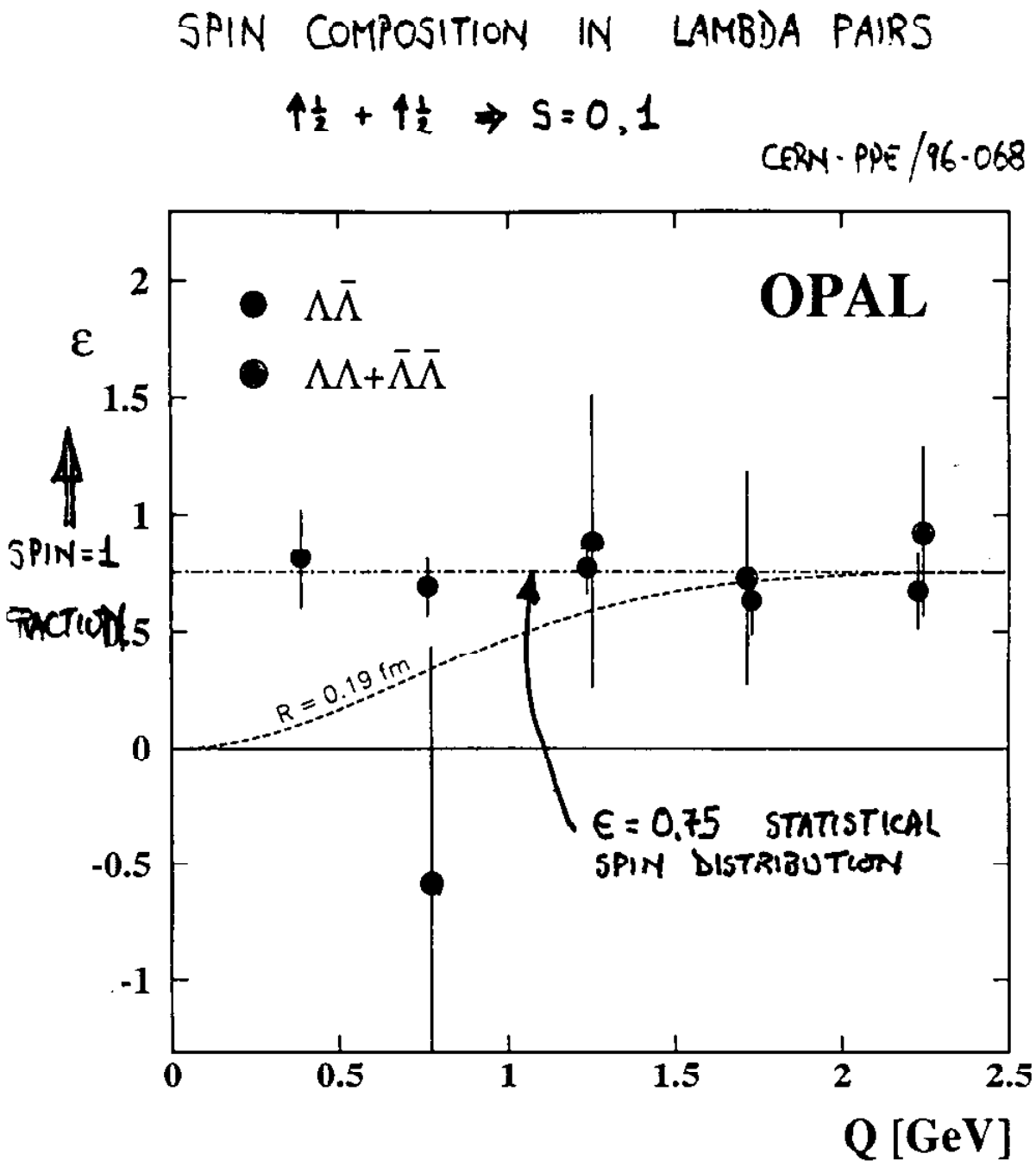

Figure 4: *The measured fraction ϵ of the $S = 1$ state contributions to the di-Λ systems as a function of Q. The full circles are for the $\Lambda\bar{\Lambda}$ sample, and the open circles are for the combined $\Lambda\Lambda$ and $\bar{\Lambda}\bar{\Lambda}$ sample. The error bars represent the statistical and systematic errors added in quadrature. The $\epsilon = 0.75$ dot-dashed line represents the statistical spin distribution. The dashed line describes the Pauli exclusion effect for an emitter radius of 0.19 fm obtained in an unbinned maximum likelihood fit to the combined $\Lambda\Lambda$ and $\bar{\Lambda}\bar{\Lambda}$ sample (see text).*

RAPIDITY CORRELATIONS IN N-BARYON SYSTEM

CERN-PPE/97-27

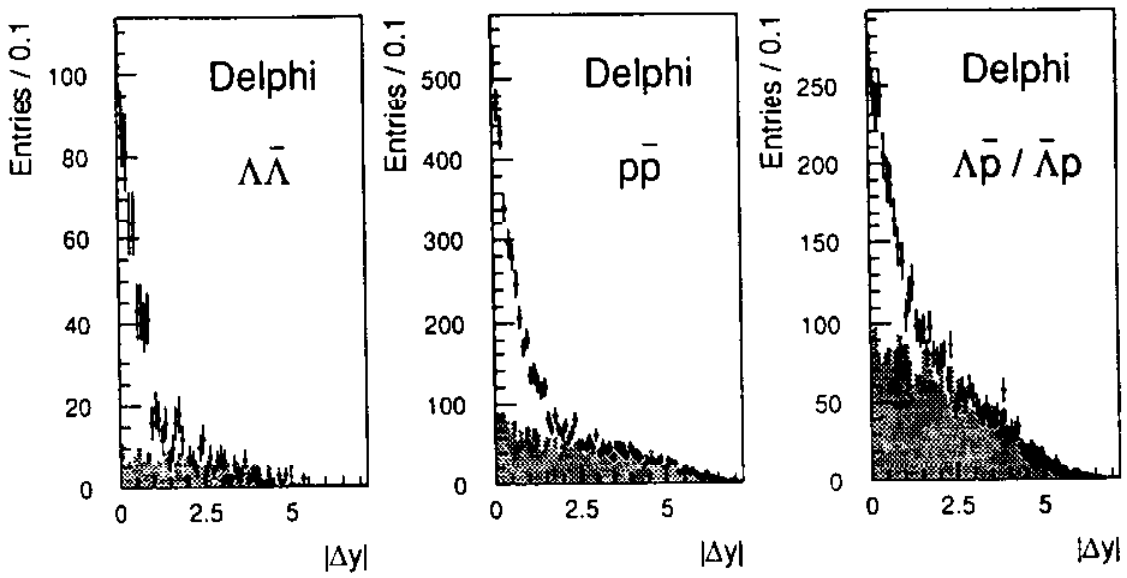

Figure 4: Rapidity differences of baryon-antibaryon pairs (points with error bars) compared to those of baryon-baryon and antibaryon-antibaryon pairs (shaded histograms) from DELPHI data.

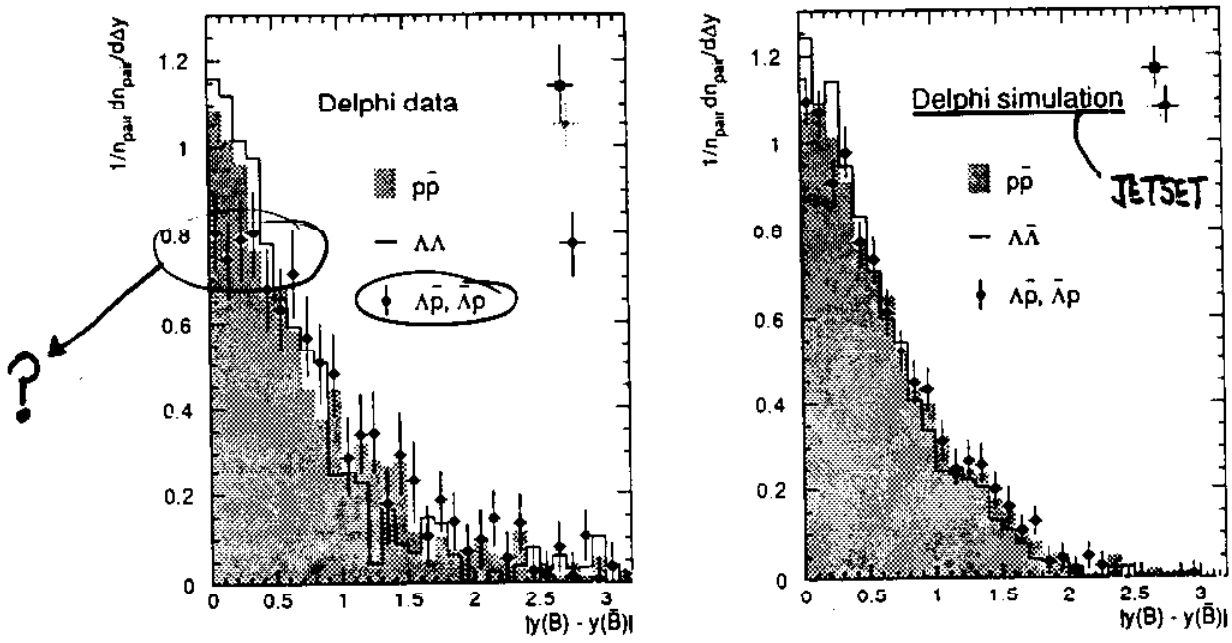

Figure 5: Rapidity differences of baryon-antibaryon pairs for real data and full JETSET 7.3 simulation with DELPHI tuning [12]. The three points with error bars on the far right of each plot show the mean values of the two leftmost bins ($|y(\mathrm{B}) - y(\overline{\mathrm{B}})| < 0.2$), referred to as peak heights in Table 2, for the three $\mathrm{B}\overline{\mathrm{B}}$ combinations, to show the significance of the effect.

ANGULAR CORRELATIONS IN Λ-BARYON SYSTEM

$p\bar{p}$ PAIRS

ALEPH

- CERN-PPE/96-186

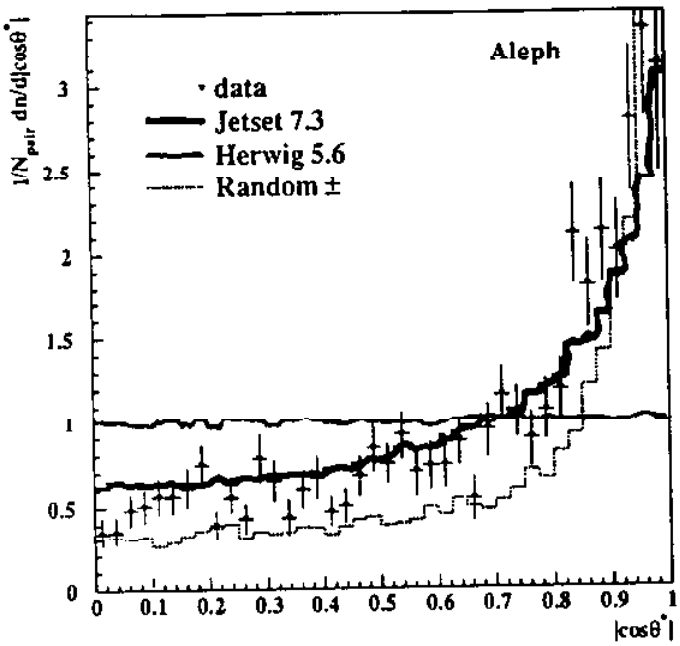

Figure 80: Like-sign subtracted, corrected $|\cos\theta^*|$ distribution of proton-antiproton pairs. θ^* is the angle between proton and sphericity axis in the proton-antiproton rest frame. The errors shown are statistical. Superimposed are the predictions of JETSET and HERWIG and the distribution for randomly-chosen unlike-sign pairs taken from JETSET. The histograms are normalized to unit area.

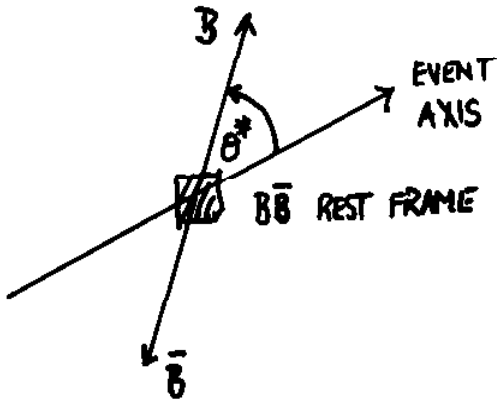

$\Lambda\bar{\Lambda}$ PAIRS

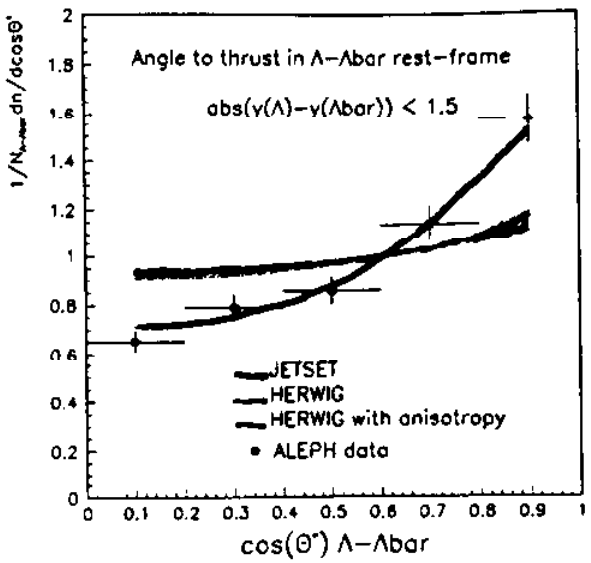

Figure 84: Angle of Λ to thrust axis in the $\Lambda\bar{\Lambda}$ rest frame, for $|\Delta y| < 1.5$.

COMPARISON WITH MODELS

BEWARE ! [1] MANY RELEASED (OFFICIAL) VERSIONS OF JETSET & HERWIG
(presumably, latest is best)
[2] COLLABORATIONS 'tune' EACH VERSION TO 'their' DATA
(presumably, latest is best)
[3] PARTICLE LISTS + DECAY BRs JETSET ≠ HERWIG in general
(presumably, latest is best)

OPAL TUNE : JETSET 7.4 + MOPS vs HERWIG 59
with identical Particle Lists + BRs

- tune EVENT SHAPES, FRAG. Fns, INCLUSIVE RATES, $\langle x_p^c \rangle$, $\langle x_p^b \rangle$, ...

⇒ Rating JETSET 7.4 + MOPS = A⁻ HERWIG 59 = B

JETSET HERWIG

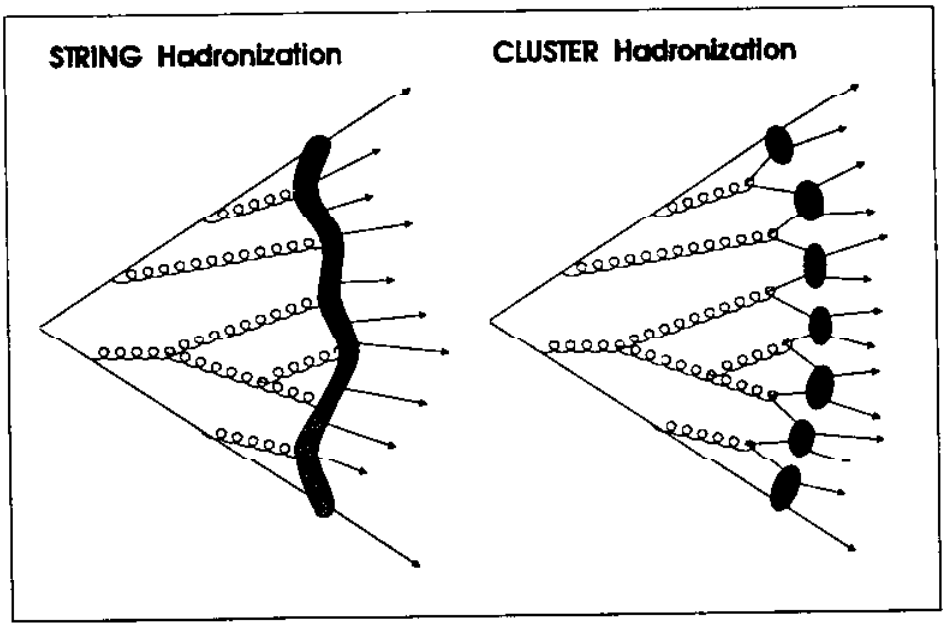

Figure 2.6: *Illustration of the string and cluster fragmentation [64].*

NEW MODEL FOR BARYON FORMATION IN JETSET

- PATRIK EDEN + GOSTA GUSTAFSON LU-TP-96-20 → Z.Phys.C.
- PATRIK EDEN LU-TP-96-29

Replaces the old POPCORN implementation in JETSET and

→ gives improved description of baryon data

EXAMPLE : SOFTENING OF BARYON FRAGMENTATION

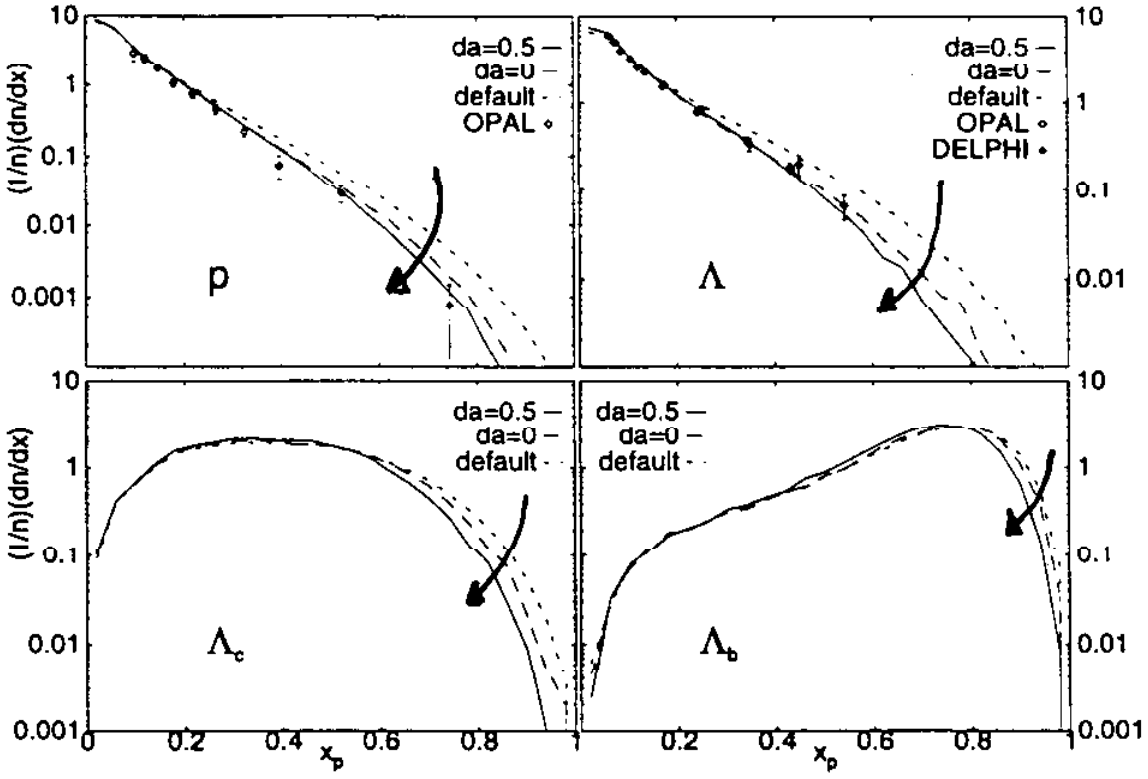

Figure 9: *Momentum distribution* $\frac{1}{n}\frac{dn}{dx_p}$ *for* p, Λ, Λ_c *and* Λ_b. $x_p = p_{\text{hadron}}/p_{\text{beam}}$. *Results from Monte Carlo simulations with* Γ *suppression model are shown for two different values of* δa, *and compared to JETSET default and experiments. OPAL data are from refs* [15]. *DELPHI data are from ref* [17].

CONCLUSIONS

[1] EXTENSIVE, GOOD PRECISION, INCLUSIVE SPECTRA at $\sqrt{s} \sim M_{Z^0}$

..... continues with full LEP1 statistics

[2] EMPHASIS NOW TURNING TO SPECIALISED STUDIES

- flavour dependence
- quark-gluon differences
- spin effects
- 2-particle correlations, eg. baryon-$\overline{\text{baryon}}$

} → better understanding of hadronisation mechanisms.

[3] JETSET + MOPS LOOKS LIKE THE WINNER